Food Chemistry: X 29 (2025) 102828

Contents lists available at ScienceDirect

Food Chemistry: X

journal homepage: www.sciencedirect.com/journal/food-chemistry-x

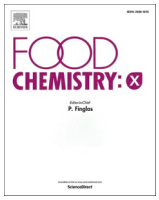

Multivariate analysis of FT-IR, bioactive compounds, and antioxidant activity in coffee pulp (*Coffea arabica* var. Catimor): combined effects of ripening stage and drying method

Alicia María Rendón-Mera [a,*], Carolina Vega-Oliveros [a,b], Sandrith Ordoñez-Lozano [a], Daniela Martínez López [a,c], Nelson Gutiérrez Guzmán [a]

[a] Centro Surcolombiano de Investigación en Café (CESURCAFÉ), Departamento de Ingeniería Agrícola, Universidad Surcolombiana, Neiva, Huila, Colombia
[b] Grupo de Investigación en Química de Hongos Macromicetos Colombianos, Departamento de Química, Universidad Nacional de Colombia, Bogotá, Colombia
[c] Universitat Politècnica de València, Departamento de tecnología de alimentos, Valencia, Spain

ARTICLE INFO

Keywords:
Coffee pulp
Ripening
Drying methods
Antioxidant capacity
Bioactive compounds
FT-IR

ABSTRACT

Coffee pulp, a nutrient-rich by-product, holds untapped nutraceutical potential but requires postharvest optimization. This study evaluated how ripening stage and drying method jointly modulate bioactive compounds in *Coffea arabica* var. Catimor pulp. FT-IR spectroscopy, HPLC-DAD, and antioxidant assays, coupled with multivariate analysis, revealed drying as the primary driver of compositional changes. FT-IR PCA (97.5 % variance in PC1) distinguished freeze-dried from thermally treated samples, while key VIP bands associated with lignin and structural carbohydrates, together with bioactive profiles (chlorogenic acid, ABTS, caffeine), revealed thermal degradation as a unifying process shaped by ripening stage. Drying × ripening effects modulated all variables except caffeine, which declined with ripening. Thermal treatments reduced phenolics, DPPH, trigonelline, and 5-CQA, with greater losses in overripe pulp. ABTS increased with roasting, while peak levels occurred in ripe freeze-dried samples. These results underscore the need for ripening-specific drying protocols to optimize coffee pulp's functional quality.

1. Introduction

Coffee is a globally significant product, valued for its sensory complexity, economic importance, and cultural impact. However, its production chain generates a considerable amount of waste at every stage, from harvesting to final preparation. These by-products possess chemical and functional properties that can be exploited for various industrial applications, including food-related uses. The valorization of these abundant residues aims to repurpose by-products generated during coffee processing, with pulp standing out as one of the most prominent. This strategy contributes to fostering a circular economy in the coffee sector by facilitating the development of new food applications with added value (Hu, Gil-Ramírez, et al., 2023). Furthermore, multiple studies have shown that coffee pulp contains significant concentrations of antioxidants, proteins, and minerals with health benefits for consumers. Altogether, these characteristics position it as a functional raw material capable of enhancing the sustainability of the coffee agro-industrial chain while reducing the environmental impact associated with waste generation (Hasballah et al., 2022).

Coffee is primarily processed through three methods: dry (natural), semi-dry (honey), and wet (washed). The latter, most used in Colombia, generates large amounts of pulp as a by-product of the mechanical depulping of coffee cherries. The pulp obtained through coffee depulping comprises a significant portion of the fruit and represents approximately 29 % of its dry matter. It is characterized by a high content of bioactive compounds, including phenolic compounds (1.5 %, encompassing hydroxycinnamic acids, flavanols, flavonols, and anthocyanidins, tannins, 1.5 %) and caffeine (1.3 %), dietary fiber (21–28 %), proteins (8–17 %), lipids (0.5–2 %), minerals (8–9.5 %), and total carbohydrates (58–85 %) (Rebollo-Hernanz et al., 2023). This combination of compounds gives the pulp antioxidant, anti-inflammatory, anti-aging, and antimicrobial properties, making it an attractive food ingredient or product that also contributes to improving consumer health (Hu, Liu, et al., 2023).

Due to its nutritional and functional properties, coffee pulp has high potential for use in the food industry. Fresh pulp, for instance, can be

* Corresponding author.
E-mail address: alisrendon@gmail.com (A.M. Rendón-Mera).

https://doi.org/10.1016/j.fochx.2025.102828
Received 29 May 2025; Received in revised form 19 July 2025; Accepted 22 July 2025
Available online 23 July 2025

easily processed into products such as jams, juices, concentrates, jellies, and flavorings. Unlike other plant-based ingredients that require purification processes to ensure a uniform chemical composition, coffee pulp allows for applications where such steps are unnecessary. Moreover, in its dried form, it has been used as flour for producing bread, cookies, muffins, brownies, snacks, pasta, cereals, sauces, and beverages. This minimal processing approach facilitates the valorization of this by-product as an innovative, accessible, and low-cost functional food (Král et al., 2024).

Coffee pulp, a by-product obtained from the wet processing of coffee cherries, accounts for between 40 % and 50 % of the fresh weight of the fruit. Its richness in nutrients and bioactive compounds has sparked interest in its use in the food, nutraceutical, and cosmetic industries, where it is valued as a natural, economically viable functional ingredient (Hasballah et al., 2022). Additionally, its health-promoting effects, supported by various biological activities, reinforce its profile as a promising bioactive ingredient. However, it is important to note that the chemical composition and antioxidant activity of pulp may vary depending on the species, variety, and maturity stage of the fruit (Hu, Gil-Ramírez, et al., 2023).

Currently, coffee pulp remains an abundant yet underutilized by-product within the coffee production chain. Its effective valorization requires not only leveraging its versatility in food applications but also enhancing its use as a nutraceutical ingredient targeted at higher value-added markets. To achieve this, it is essential to understand how factors such as fruit maturity and processing conditions, particularly the drying method, modulate its bioactive composition and functional properties.

Given its high moisture content (above 80 %), the stabilization of coffee pulp requires effective drying processes to prevent the degradation of phytochemicals, reduce water activity, and minimize microbiological risks, thereby extending its shelf life and enabling its incorporation as a stable, versatile, and easily transportable functional ingredient (Hu, Liu, et al., 2023; Jiamjariyatam et al., 2022; Kieu Tran et al., 2020). Several studies have shown that the drying method significantly affects the preservation of key bioactive compounds as well as the functional properties of coffee pulp (Lu et al., 2023; Mesfin et al., 2023).

In this context, three contrasting drying techniques were selected: freeze-drying, for its capacity to preserve heat-sensitive metabolites (Hu, Gil-Ramírez, et al., 2023; Jiamjariyatam et al., 2022); oven drying, for its accessibility and industrial scalability; and roasting, for its ability to induce relevant chemical transformations, such as the formation of melanoidins, which are associated with functional benefits (Mesfin et al., 2023). This selection responds to the need to identify treatments that balance low cost with high bioactive potential.

Additionally, the degree of cherry maturity has been identified as a critical factor influencing the concentration of compounds such as sugars, organic acids, phenolic compounds, and alkaloids, which may affect the functional potential of the pulp (Bi et al., 2024). Harnessing this potential requires understanding how maturity stage interacts with drying method, enabling the optimization of postharvest strategies that maximize the bioactivity of the final product. This knowledge is crucial not only for guiding technical processing decisions but also for supporting value generation in coffee-growing regions, promoting more equitable and sustainable supply chains.

To date, no studies have systematically analyzed how ripening stage and drying method influence the chemical composition and functional potential of coffee pulp. Therefore, this study aimed to characterize their combined effects on the antioxidant capacity, bioactive compound profile, and FT-IR spectral features of *Coffea arabica* var. Catimor pulp. Specifically, it sought to evaluate how ripening stage influences the content and antioxidant activity of key bioactive compounds, assess the impact of different drying methods on their preservation and transformation, and identify discriminant FT-IR spectral markers associated with these processing treatments through an integrated multivariate approach. This preliminary yet comprehensive assessment lays the groundwork for future metabolomic studies and industrial-scale validations, providing foundational knowledge to guide valorization strategies for coffee pulp as a functional food or nutraceutical ingredient.

2. Material and methods

2.1. Reagents and standards

The solvents, reagents, and reference compounds used in this study were sourced from Loba Chemie PVT. LTD. (India), PanReac AppliChem (Germany), Merck (USA), and Sigma-Aldrich (India, Switzerland, and China). All solvents were HPLC grade, including methanol (Loba Chemie PVT. LTD.). Analytical standards included gallic acid (≥ 99 %, HPLC grade), Trolox, caffeine, and chlorogenic acid (≥ 95 %, by titration), all supplied by Sigma-Aldrich. For spectrophotometric assays, Folin–Ciocalteu reagent (PanReac AppliChem), sodium carbonate, and potassium persulfate (≥ 98 %) were obtained from Loba Chemie PVT. LTD., and ABTS (≥ 98 %, HPLC grade) from Merck. All reagents were handled and stored according to the manufacturers' instructions until use.

2.2. Processing, maturity sorting, and drying

Catimor variety coffee cherries (*Coffea arabica* var. Catimor) were hand-harvested on June 11, 2024, from the "Varietales Exóticos" production unit (UPA) located in the rural settlement (vereda) "La Siberia", Acevedo municipality, Huila, Colombia (1°44′37.2"N, 76°00′15.1"W). This UPA encompasses an area of approximately 18–20 ha, dedicated to various coffee varieties and cultivation activities. The specific cherries used in this study were collected at an altitude of 1670.6 m a.s.l. All cherries were sourced from a single lot and farm to ensure homogeneity and to maintain constant environmental variables such as altitude, climate, and soil conditions, which could otherwise affect metabolite profiles. Harvesting and transport occurred on the same day, with cherries sent directly to the Cesurcafé facility at Universidad Surcolombiana in Neiva (~5 h transit) for immediate processing. For transportation, expanded polystyrene (EPS) coolers were used to prevent physical, chemical, or microbiological cross-contamination, and cold gel packs were placed inside to maintain the temperature below 8 °C, thereby minimizing postharvest fermentation of the cherries and preserving pulp integrity. Upon arrival, cherries were washed, floaters removed, and disinfected by immersion in a Timsen® solution (1 g/L; 40 % alkyl benzyl quaternary ammonium and 60 % chelated urea; food-grade). Only healthy cherries were selected within each ripeness category. They were manually sorted by color into three maturity stages: unripe (green and yellowish), ripe (red), and overripe (damaged or dark red to black), following the visual scale shown in Fig. 1. Peduncles were removed during sorting to avoid potential off-flavors during subsequent processing and product development.

Depulping was performed separately for each ripeness category using a depulper (GAVIOTA MDZ 300, 300 kg/h, INGESEC-PROMAIN LTDA, Colombia). The harvest batch consisted of approximately 150 kg of Catimor cherries, which were sorted by ripeness stage. From the total pulp yield, representative subsamples of approximately 2 kg of pulp per ripeness stage were collected for this study, corresponding to ~5 kg of whole coffee cherries per ripeness stage based on an average pulp yield factor of 0.4, estimated from yields measured during sample processing. These subsamples were immediately subjected to dehydration via freeze-drying or oven-drying, following a 3 × 3 factorial experimental design comprising three ripening stages (unripe, ripe, overripe) and three drying methods (freeze-drying, oven-drying, roasting), with three biological replicates per treatment.

2.3. Drying procedures

For freeze-drying, pulp samples sorted by maturity were first frozen

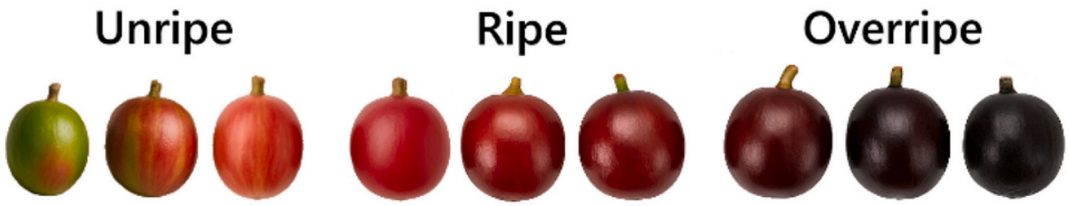

Fig. 1. Visual scale used to classify coffee cherries by maturity stage (Unripe, Ripe, and Overripe). Digital illustration based on reference material.

at −80 °C in an ultra-freezer (Haier Biomedical, ULT DW-86L338J, China) and then processed in a freeze-dryer (Biobase®, BK-FD12P, China) for 48 h. The dried samples were stored again at −80 °C until analysis.

For oven-drying, pulp samples were dried separately by maturity stage in convection ovens (Memmert GmbH, UF55 and UF110, Germany) at 50 °C, with the vent fully open (100 %) and fan at 100 %. Manual stirring and tray rotation were performed every 20 min during the first 4 h. Subsequently, the vent was adjusted to 80 % open and fan speed reduced to 50 %, with homogenization every 2 h until reaching a moisture content of 7–10 %. Moisture was monitored using an infrared moisture analyzer (RADWAG MA 50.X2.A, Poland).

Half of each oven-dried pulp sample was roasted using a laboratory roaster (DIBAR®, MD-150, Colombia) at an inlet temperature of 110 °C, with closed heat curtain and 20 % flame. The tipping point (100 °C) was reached at 1 min 10 s, and the roast was completed at 110 °C after a total duration of 10 min.

All samples were then ground using a coffee grinder (Hamilton Beach®, model 80,393, USA) and sieved through a stainless-steel mesh (35 mesh, 500 μm) according to ASTM E11 standards. Moisture content was determined by drying at 105 °C to constant weight, following ISO 6673:2003 (green coffee), using approximately 1 g of dried pulp. The processed samples were stored in desiccators, in high-density polyethylene (HDPE) bags, at room temperature for a maximum of one month until extraction or further analyses. Thus, for each maturity stage (unripe, ripe, and overripe), three types of pulp samples were prepared: freeze-dried, oven-dried, and roasted.

2.4. FT-IR spectroscopic analysis of coffee pulp samples

FT-IR measurements were performed on approximately 1 g of the previously ground and sieved pulp samples (oven-dried, freeze-dried, and/or roasted) described above. Measurements were carried out using an Cary 630 FT-IR spectrophotometer (Agilent Technologies, USA) equipped with a horizontal attenuated total reflectance (ATR) accessory featuring a diamond crystal. Samples were placed in the ATR accessory and compressed. Spectra were collected in the range of 4000–650 cm^{-1} with a resolution of 8 cm^{-1} and 32 scans under controlled ambient conditions (~20 ± 0.5 °C). Background readings were acquired prior to each measurement under identical conditions. Raw spectra were pre-processed to enhance comparability among samples using baseline correction, standard normal variate (SNV), and first and second derivative transformations, and then exported to Excel for further analysis. A total of 45 biological samples (3 ripening stages × 3 drying methods × 5 replicates) were analyzed. Each replicate corresponded to an independently processed pulp sample subjected to the full drying and grinding protocol, following the methodology reported by Barrios-Rodríguez et al. (2021).

2.5. Preparation of methanolic extracts

Ground and sieved pulp samples were extracted using a 50:50 water: methanol system with heating in an ultrasonic bath (Elma S 30 – Elmasonic, Germany). For each sample, 250 mg of pulp were weighed into 50 mL plastic tubes, and 40 mL of the water/methanol mixture were added. The mixture was homogenized using a vortex (Heidolph Reax Top Shaker, Germany) and sonicated at 60 °C for 30 min. Extracts were centrifuged at 4500 rpm for 5 min (Ortoalresa–Bioprocen 22 R, Spain), filtered through Whatman No. 4 paper, and the final volume was adjusted to 50 mL with the 50:50 water/methanol mixture. Prepared extracts were stored at −18 °C until spectrophotometric and HPLC-DAD analyses to preserve compound stability.

2.6. Spectrophotometric determination of Total phenolic compounds

Total phenolic content was determined using the Folin–Ciocalteu colorimetric method based on Myo and Khat-udomkiri (2022) with modifications. Briefly, 2400 μL of distilled water and 100 μL of Folin–Ciocalteu reagent were mixed in a test tube, followed by 250 μL of pulp methanolic extract or blank. Tubes were vortexed and incubated for 6 min. Then, 2000 μL of 2 % sodium carbonate solution were added, mixed, and incubated in the dark for 120 min. Absorbance was measured at 750 nm using a spectrophotometer (UV–Vis, Thermo Scientific-GenesysTM 180, Ireland). A total of 27 biological samples (3 ripening stages × 3 drying methods × 3 replicates) were analyzed. Each extract was measured in quadruplicate (technical replicates) to assess intra-assay variability and improve analytical precision (Apak et al., 2016; Myo & Khat-udomkiri, 2022). Quantification was based on a calibration curve using gallic acid as the standard, and results were expressed as mg gallic acid equivalents per 100 g of coffee pulp (mg GAE/100 g). Each calibration point was also measured in quadruplicate, and reagent blanks were included in each batch. Calibration curve data and method precision (RSD) are provided in Supplementary Material Table S3.

2.7. ABTS radical scavenging assay

The protocol from Myo and Khat-udomkiri (2022) was adapted slightly for use in the ABTS radical scavenging assay. Pulp methanolic extracts were mixed with activated ABTS solution (7 mM) prepared with potassium persulfate (2.45 mM, 98 %). A volume of 20 μL of each extract was mixed with 2000 μL of activated ABTS solution, and absorbance was measured at 734 nm. The ABTS radical optical density was verified at 0.700 ± 0.015. After a 6-min incubation in the dark, inhibition was measured spectrophotometrically. A total of 27 biological samples were analyzed in quadruplicate (see Section 2.6). Quantification was based on a Trolox calibration curve, and results were expressed as μmol Trolox equivalents per gram of coffee pulp (μmol TE/g). Each calibration point was also measured in quadruplicate. Reagent blanks and cell blanks were included in each batch for baseline correction. Calibration curve data and method precision (RSD) are provided in Supplementary Material Table S3.

2.8. DPPH radical scavenging assay

The DPPH radical scavenging assay was conducted using a slightly modified version of the protocol outlined by Myo and Khat-udomkiri (2022). Methanolic extracts were mixed with activated DPPH solution, incubated in the dark, and the inhibition of the radical was measured spectrophotometrically at 517 nm. Each assay included 27 biological

samples analyzed in quadruplicate (see Section 2.6). Antioxidant capacity was calculated from a Trolox standard curve and reported as μmol Trolox equivalents per gram of coffee pulp (μmol TE/g). All calibration points were prepared and read in quadruplicate, and both reagent and cell blanks were included in each run. Additional details, including curve parameters and intra-assay precision, are provided in Supplementary Material Table S3.

2.9. HPLC-DAD analysis of caffeine, trigonelline, and chlorogenic compounds in coffee pulp

One-milliliter aliquots of the methanolic extracts were taken for chromatographic analysis. Each aliquot was filtered through a 0.45 μm nylon syringe filter and transferred to amber vials, then kept at 4 °C until analysis using HPLC (Agilent Technologies 1260 Infinity II, USA). Caffeine and trigonelline quantification was performed using a 1260 Infinity HPLC system equipped with a quaternary pump, autosampler, column thermostat, and DAD detector (Agilent, Waldbronn, Germany). The procedure was based on Oteef (2022), with modifications. The gradient started with 80 % phase A (water acidified with 1 % acetic acid) and 20 % phase B (methanol), held for 1 min; adjusted to 75 % A/25 % B until 3.5 min; then transitioned to 0 % A/100 % B from 4 to 8 min; and returned to 80 % A/20 % B, stabilized until 11 min. Injection volume was 10 μL, flow rate 1 mL/min, and column temperature 30 °C. Detection was set at 272 nm for caffeine and trigonelline and at 325 nm for chlorogenic acids. Identification and quantification were based on retention time and calibration curves using caffeine and chlorogenic acid standards. Analyses were performed on 27 samples (three ripening stages × three drying methods × three biological replicates), with each extract injected once. Method performance was monitored throughout the sequence by including calibration standards every 10 injections (20, 50, and 80 ppm), procedural blanks, and randomly selected samples enriched to evaluate spiked recovery, along with their duplicates to assess precision. Parameters, including calibration curve data, intra-assay precision (RSD), and quality control results, are provided in Supplementary Material Table S3.

2.10. Statistical analysis

All statistical analyses were performed in R version 4.4.3. Univariate analyses were conducted to assess the effects of experimental factors on each response variable. Assumptions of normality (Shapiro–Wilk test), homogeneity of variances (Levene's test), and data independence (verified using graphical methods) were checked. Variables meeting all three assumptions were analyzed by one-way ANOVA ($\alpha = 0.05$), followed by Tukey's HSD and Fisher's LSD post hoc comparisons. For variables that did not meet assumptions, even after transformation, the Kruskal–Wallis test was applied, followed by Dunn's multiple comparison test with Bonferroni adjustment, implemented using the FSA package. In such cases, to evaluate interactions, a linear regression model with HC3 robust standard errors was fitted. Additionally, for IR spectra, the latent variable PC1, obtained through principal component analysis (PCA), was used to conduct the aforementioned analyses.

For multivariate analysis, the data were divided into extract datasets (UV–Vis and HPLC-DAD) and FT-IR spectra datasets. Both unsupervised and supervised multivariate techniques were applied. PCA was first used to reduce dimensionality and identify natural groupings associated with experimental factors.

In both datasets, this was complemented by supervised models (PLS-DA), developed using the *plsda()* function from the mixOmics package. Prior to modelling, datasets were mean-centered and scaled to unit variance. PLS-DA models were validated via M-fold cross-validation (5 folds, 50 repetitions) with a random seed set for reproducibility. Model performance was evaluated based on explained variance (R^2X and R^2Y), predictive capacity (Q^2), area under the ROC curve (AUC), and classification error rates (using Mahalanobis distance). These metrics guided the selection of the optimal number of components for each model.

For FT-IR data ($n = 45$), different spectral preprocessing strategies were compared, specifically evaluating raw spectra, first derivative, and second derivative transformations. The first derivative was selected due to its superior discriminative performance in PLS-DA models. Variable selection for subsequent sPLS-DA models considered the top five VIP-ranked variables per component (three components per factor) from each PLS-DA model (ripening stage and drying method). This approach ensured inclusion of the most discriminant wavenumbers across both experimental factors while maintaining the number of variables below the total sample size (n = 45), thus minimizing overfitting risk. The initial set of 30 variables was reduced to 25 unique variables after removing duplicates.

sPLS-DA models were then developed using the *splsda()* function, applying the same validation strategy (M-fold cross-validation with 5 folds and 50 repetitions). Model performance was evaluated based on R^2X, R^2Y, Q^2, AUC, and classification error rates, ensuring comparability with PLS-DA results. This approach improved class separation while preserving model stability, consistent with the exploratory objectives of this study.

3. Results and discussion

3.1. FT-IR spectroscopic analysis of coffee pulp composition

The Fourier-transform infrared (FT-IR) spectral analysis provides detailed information on the functional groups present in coffee pulp, enabling the characterization of its major chemical components and structural features. Spectra were recorded across the 650–4000 cm^{-1} range. Fig. 2 displays a representative spectrum of the analyzed samples. Table 1 summarizes the most prominent peaks, indicating for each the wavenumber and a concise description encompassing both the vibrational assignment (e.g., O—H, C—H, C═O stretching or aromatic deformations) and the key chemical components involved (cellulose, hemicellulose, lignin, phenolics, alkaloids). These functional groups reflect the pulp's richness in polysaccharides, lignin derivatives, and phenolic esters, which are relevant for its structural integrity and bioactive potential. This facilitates a rapid and comprehensive interpretation of the pulp's spectral signature in the context of ripening and thermal processing effects explored in this study.

To quantify the spectral differences attributable to ripeness stage and drying method (freeze-drying, oven-drying, and roasting), multivariate tools were applied. First, principal component analysis (PCA) was performed to identify the main sources of variation; subsequently, Kruskal–Wallis tests and robust regressions with HC3 estimators were conducted on the first principal component (PC1) to assess the effect of the experimental factors. Thereafter, sparse partial least squares discriminant analysis (sPLS-DA) was used to identify the FT-IR bands that most effectively discriminated between treatments. The results are detailed in the following sections.

3.1.1. Dimensionality reduction of spectral data via PCA

Principal component analysis (PCA) was applied to the centered and scaled FT-IR spectra in the 1800–645 cm^{-1} region (fingerprint region), where most characteristic bands are concentrated. The first two components explained 97.5 % (PC1) and 1.55 % (PC2) of the total variance, with PC1 representing the main axis of separation. In the score plot, the freeze-dried samples (VL, ML, SML) clustered in the negative PC1 and PC2 region, whereas oven-dried (VS, MS, SMS) and roasted samples (VT, MT, SMT) appeared with positive PC1 values (Fig. 3). This pattern suggests marked differences in chemical composition associated with the type of treatment: samples subjected to freeze-drying, which better preserve the original matrix, grouped at the negative end of PC1, while those exposed to thermal treatments—oven-drying and roasting—shifted toward positive values, reflecting evident spectral transformations. (See Fig. 4.)

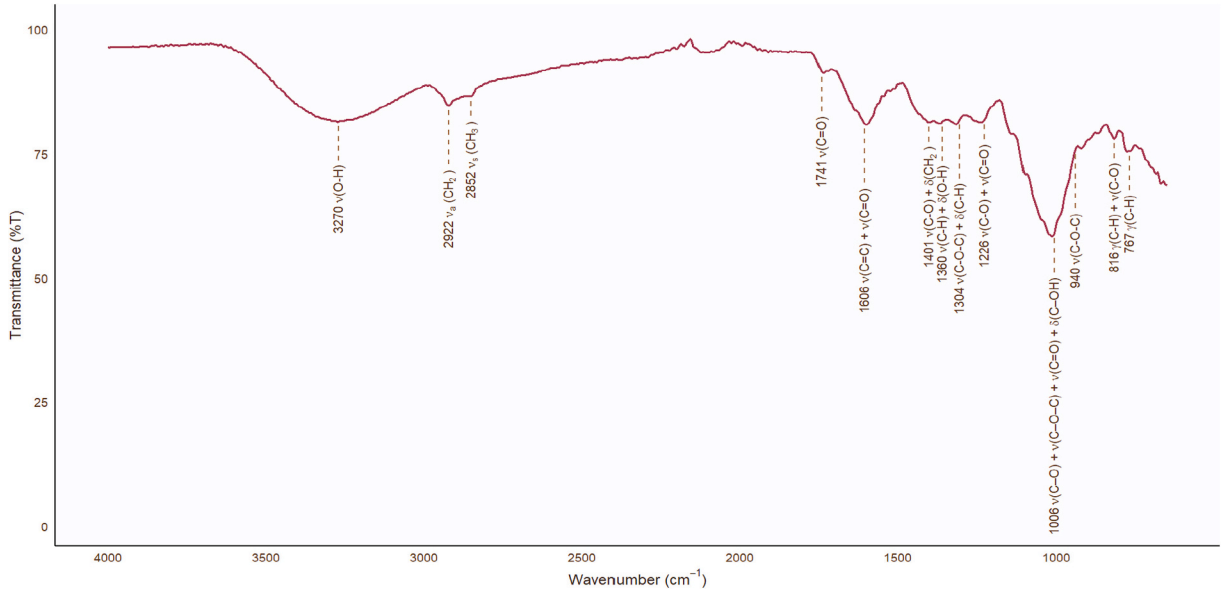

Fig. 2. Representative IR spectrum of dried coffee pulp samples.

Since PCA captures unsupervised natural variance patterns, the loading analysis allows identification of the spectral bands contributing most to the overall variability among samples, primarily associated with differences in ripeness and thermal processing. To identify these relevant spectral variables, we selected the most prominent peaks (maxima and minima) in the loading plots of PC1 and PC2, following standard practice in multivariate FT-IR analysis. The loading analysis revealed that the predominant chemical differences were mainly related to structural changes induced by thermal processing. In both PC1 and PC2, major contributions were observed from bands at 1725, 1707, 1569, 1180, 1032, and 984 cm^{-1}, while PC2 also included signals at 1443, 1397, 1331, 1274, 1145, 795, and 754 cm^{-1}. Full vibrational assignments, including functional group attributions and literature references for these bands, are detailed in Supplementary Table S1.

In PC1, the carbonyl bands (1725 and 1707 cm^{-1}) indicate lipid degradation, formation of new esters, and oxidation of thermolabile compounds (Belchior et al., 2020; Iriondo-DeHond et al., 2019; Oliveira et al., 2018). The signal at 1569 cm^{-1} reflects alterations in lignin and proteins (Jiménez-Ochoa et al., 2022; Oliveira et al., 2018), while the bands at 1180 and 1032 cm^{-1} point to changes in structural carbohydrates and chlorogenic acid esters (Liang et al., 2016; Oliveira et al., 2018; Zeleke et al., 2022). Finally, the band at 984 cm^{-1} corresponds to cell wall polysaccharides (Barrios-Rodríguez et al., 2021; Belchior et al., 2020). These signals suggest that PC1 functions as a thermal severity axis, where the intensification of carbonyl, ester, and polysaccharide bands reflects lipid degradation, metabolite oxidation, and carbohydrate breakdown as thermal treatment intensity increases.

PC2 additionally incorporated bands at 1443 and 1397 cm^{-1} associated with lignin and chlorogenic acids (Oliveira et al., 2018; Zeleke et al., 2022); 1145 cm^{-1}, linked to hemicellulose and chlorogenic acid (CGA) signatures (Jiménez-Ochoa et al., 2022; Liang et al., 2016; Oliveira et al., 2018; Zeleke et al., 2022); 1331 and 1274 cm^{-1} characteristic of guaiacyl/syringyl lignin rings and CGA (Oliveira et al., 2018; Veiga et al., 2017); and bands at 795 and 754 cm^{-1}, reflecting aromatic deformations in lignin (Liang et al., 2016; Oliveira et al., 2018; Taleb et al., 2020). This suggests that PC2 captures more specific alterations in the lignocellulosic matrix under different drying methods. The prominent appearance of lignin bands supports previous observations in chemically treated coffee pulp fibers, where similar structural changes were detected in FTIR spectra (Oliveira et al., 2018).

Finally, an interaction between ripeness stage and thermal processing was observed. In roasted samples, positive PC1 values progressively increased as the fruit advanced from unripe to overripe stages, indicating that higher ripeness could favor the accumulation of advanced oxidation products and the potential formation of melanoidins during heating.

3.1.2. *Statistical assessment of ripeness and drying effects on spectral signatures*

To assess the effect of ripeness and drying method on spectral variation, PC1 (97.5 % of the variance) was used as a latent variable. Since normality and homoscedasticity assumptions were not met, the Kruskal–Wallis test with Dunn–Bonferroni post hoc comparisons and a robust linear regression model (HC3 estimator) were applied.

The Kruskal–Wallis test showed significant differences by ripeness ($p = 0.019$) and by drying method ($p < 0.001$). The Dunn test revealed that only the overripe pulp differed from the ripe samples ($p = 0.016$), and that freeze-dried samples differed from both oven-dried ($p = 0.006$) and roasted samples ($p = 0.0005$), with no significant difference between oven-dried and roasted treatments.

The HC3 model confirmed these patterns and provided estimates of their magnitude: taking freeze-dried samples as the reference, roasting caused the largest shift in PC1 ($p < 0.001$), while oven-drying was marginally significant ($p = 0.051$), suggesting a trend toward intensified thermal transformations. Mesfin et al. (2023) reported that roasting disrupts lignin–phenol bonds, transforms polysaccharides and polyphenols, and generates melanoidins, altering the chemical composition and spectral signature.

Regarding ripeness, the overripe stage significantly increased PC1 values ($p = 0.042$). These results reinforce that the final stages of ripening are associated with chemical alterations detectable by FT-IR, transitioning from glycoside and flavonoid synthesis to the catabolism of secondary metabolites (Bi et al., 2024).

Interaction effects showed that in ripe fruits, roasting produced a significant decrease in PC1 ($p = 0.0018$), indicating that the combination of advanced ripeness and heat intensifies modifications of sensitive chemical components. In contrast, no significant interaction effects were observed between ripeness and oven-drying—for instance, in ripe samples ($p = 0.570$), unripe samples ($p = 0.134$), or overripe samples ($p = 0.132$)—suggesting that oven-drying only modulates the spectral profile under the more intense conditions of roasting.

Altogether, these findings demonstrate that the combination of

Table 1
FT-IR band assignment (650–4000 cm^{-1}) for Catimor coffee pulp.

Wavenumber (cm^{-1})	Description	References
3270	Broad O—H stretching of hydroxyl groups in phenolics, lignin, hemicellulose and cellulose, plus hydrogen-bonded water.	Barrios-Rodríguez et al. (2021)
2922	C–H stretching (asymmetric CH_2 and symmetric CH_3) from fatty-acid esters, methyl/methylene groups of caffeine and lignocellulosic polysaccharides.	Belchior et al. (2020); Jiménez-Ochoa et al. (2022); de Oliveira et al. (2018)
2852	Symmetric C—H stretch of methyl groups in caffeine, lignin methoxyls and lipid moieties.	Gonçalves et al., 2021; Jiménez-Ochoa et al. (2022); de Oliveira et al. (2018)
1741	C=O stretching of ester and carboxylic acid groups (triglycerides, aliphatic esters); low intensity suggests low concentration or weak absorption.	Iriondo-DeHond et al. (2019); Liang et al. (2016); Oliveira et al. (2018); Zeleke et al. (2022)
1606	Overlapping aromatic C=C and conjugated C=O stretches from chlorogenic acids, lignin aromatic rings, trigonelline and caffeine.	Barrios-Rodríguez et al. (2021); Gonçalves et al. (2021); Iriondo-DeHond et al. (2019); Liang et al. (2016); de Oliveira et al. (2018)
1401	C–O stretching and O–H/N–H bending of carbohydrates and chlorogenic-acid esters; also reflects soluble dietary fiber.	Jiménez-Ochoa et al. (2022); Veiga et al. (2017); Yu et al. (2025); Zeleke et al. (2022)
1360	C–H bending (trigonelline methyls) and C–OH stretching of crystalline cellulose; overlaps with lignin C—H deformations.	Belchior et al. (2020); Jiménez-Ochoa et al. (2022); de Oliveira et al. (2018)
1304	C–O–C/C–O stretching of chlorogenic-acid esters, polysaccharides and lignin ether linkages; phenyl-ring vibrations and O—H deformation modes.	Barrios-Rodríguez et al. (2021); Iriondo-DeHond et al. (2019); Jiménez-Ochoa et al. (2022); Liang et al. (2016); de Oliveira et al. (2018); Veiga et al. (2017)
1226	Aromatic-ring vibrations (C—C, C—O, C=O) in lignin and chlorogenic acids, plus C—O stretch in sucrose and hemicellulose.	Barrios-Rodríguez et al. (2021); Oliveira et al. (2018); Veiga et al. (2017)
1006	Overlapping C—O and C–O–C stretches of β-(1 → 4) glycosidic linkages in cellulose, hemicellulose, arabinogalactans and chlorogenic acids.	Barrios-Rodríguez et al. (2021); Belchior et al. (2020); Liang et al. (2016)
940	C–O–C glycosidic stretch of β-(1 → 4) polysaccharides (cellulose, hemicellulose); overlaps with arabinogalactan and carbohydrate signals.	Belchior et al. (2020); Yu et al. (2025) Zeleke et al. (2022)
816	C–O stretch and aromatic C—H out-of-plane bending in guaiacyl/syringyl lignin units and chlorogenic acids.	Liang et al. (2016); Oliveira et al. (2018); Taleb et al. (2020)
767	C–H out-of-plane bending in lignin aromatic rings, characteristic of the lignocellulosic matrix.	Barrios-Rodríguez et al. (2021)

advanced ripeness and thermal processing generates distinctive spectral signatures, which may guide industrial drying strategies aimed at preserving bioactive compounds in coffee pulp-derived products.

3.1.3. Discriminant models for ripening stage and drying method

Supervised PLS-DA and sPLS-DA models were subsequently applied to evaluate the discrimination of ripeness stages and drying methods. The spectra were analyzed using their first derivative to optimize model stability.

For classifying ripeness stages, the PLS-DA model adequately explained the data variance (cumulative $R^2X = 0.71$ and $R^2Y = 1.40$) but, it showed limited predictive capacity ($Q^2 = 0.18$; classification error = 32.7 %). These results indicate challenges in correctly separating ripeness groups, with performance falling below the generally accepted threshold for robust models ($Q^2 > 0.50$). In contrast, the sPLS-DA model markedly improved ripeness discrimination, maintaining satisfactory explanatory levels (cumulative $R^2X = 0.69$ and $R^2Y = 1.29$) and increasing predictive ability ($Q^2 = 0.46$; classification error = 23.2 %). AUC values were high (0.96 for "Unripe" and "Ripe", 0.95 for "Overripe"), indicating excellent separation of ripeness stages. These results demonstrate that variable selection via VIP strengthened the model's stability and robustness.

For discriminating drying treatments, the PLS-DA model adequately explained data variability (cumulative $R^2X = 0.73$ and $R^2Y = 1.30$), showing high predictive capacity ($Q^2 = 0.87$; classification error = 5.9 %). ROC curves confirmed perfect discrimination between "Freeze-dried," "Oven-dried," and "Roasted" samples (AUC = 1.00 for all classes). The sPLS-DA model, adjusted with only two components (cumulative $R^2X = 0.50$; $R^2Y = 1.00$; $Q^2 = 0.87$), exhibited a comparable overall classification error (6.1 %), also evaluated using Mahalanobis distance. The sPLS-DA model, using just two components (cumulative $R^2X = 0.50$ and $R^2Y = 1.00$), maintained comparable performance ($Q^2 = 0.87$; classification error = 6.1 %), with stability validated through cross-validation. These results confirm that variable reduction via sPLS-DA did not compromise classification performance, and it highlighting its efficiency in optimizing data dimensionality.

Fig. 5 A shows the distribution of samples by ripeness stage (Unripe, Ripe, Overripe). The first component explained 21 % of the variance, and the second component explained an additional 21 %, capturing a relevant portion of discriminative variability. The unripe samples clustered on the far left, the ripe samples in the mid-right region, and the overripe samples in the upper-right part of the plot. Although some overlap was observed between ripe and overripe samples, most grouped coherently according to their ripeness stage. These patterns reflect that the physicochemical modifications associated with the ripening process are manifested in the spectral variables selected by sPLS-DA.

Fig. 5B shows the distribution of samples by drying method: freeze-dried, oven-dried, and roasted. The first component explained 35 % of the variability, while the second component explained an additional 14 %. Three clearly differentiated groupings were observed, evidencing that each method imparts a distinct chemical signature to the coffee pulp. The freeze-dried samples, located in the left section, reflected greater preservation of volatile and thermolabile compounds due to low thermal exposure. The oven-dried samples, in the lower-right region, showed an intermediate profile, likely due to incipient browning reactions. The roasted samples, concentrated in the upper-right, exhibited deeper chemical modifications associated with Maillard and caramelization reactions (Mesfin et al., 2023). Collectively, these results highlight the effectiveness of sPLS-DA in discriminating drying treatments and underscore the impact of thermal processing on the chemical composition and nutraceutical potential of coffee pulp.

Overall, the application of sPLS-DA significantly improved discrimination capacity for both ripeness stages and drying methods, reducing dimensionality without compromising predictive performance. These findings reinforce the utility of supervised multivariate strategies to interpret physicochemical modifications induced by ripening and thermal processing in coffee pulp.

3.1.4. Discriminative FT-IR bands via VIP analysis

The sPLS-DA analysis enabled the identification of critical spectral bands (VIP > 1) that discriminate coffee pulp according to ripeness stage (unripe, ripe, and overripe) and type of thermal processing (freeze-

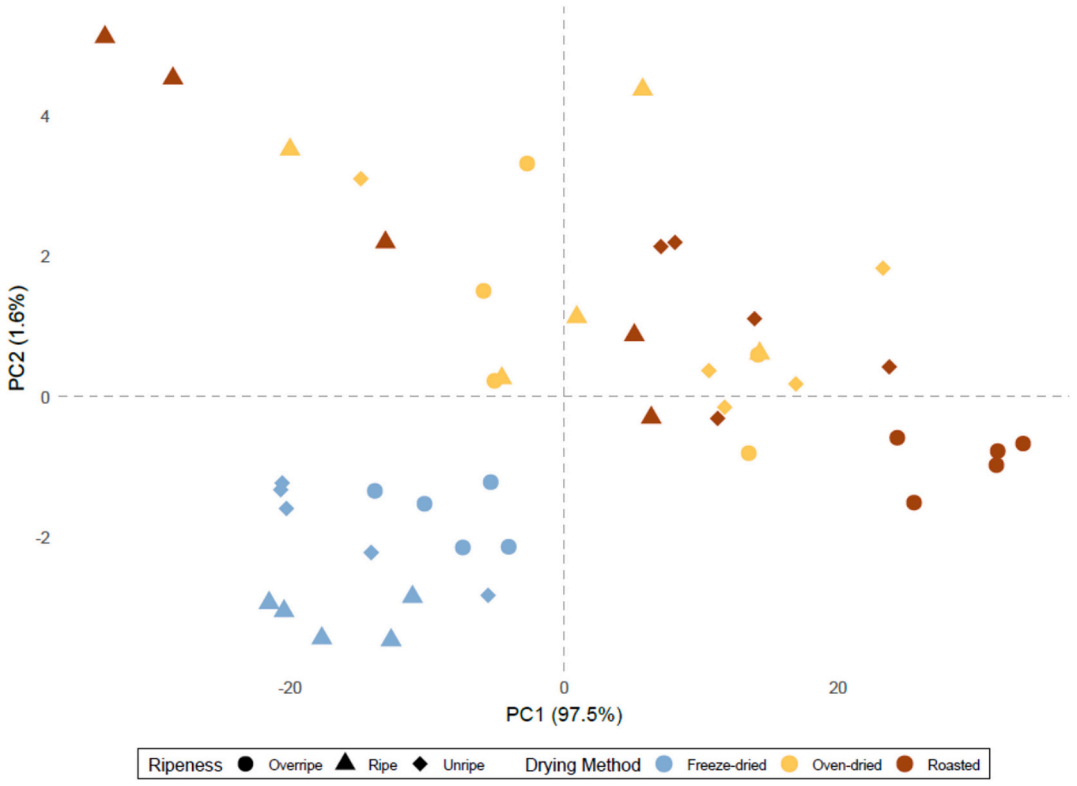

Fig. 3. Principal Component Analysis (PCA) of IR spectra grouped by ripeness stage and drying method of coffee pulp.

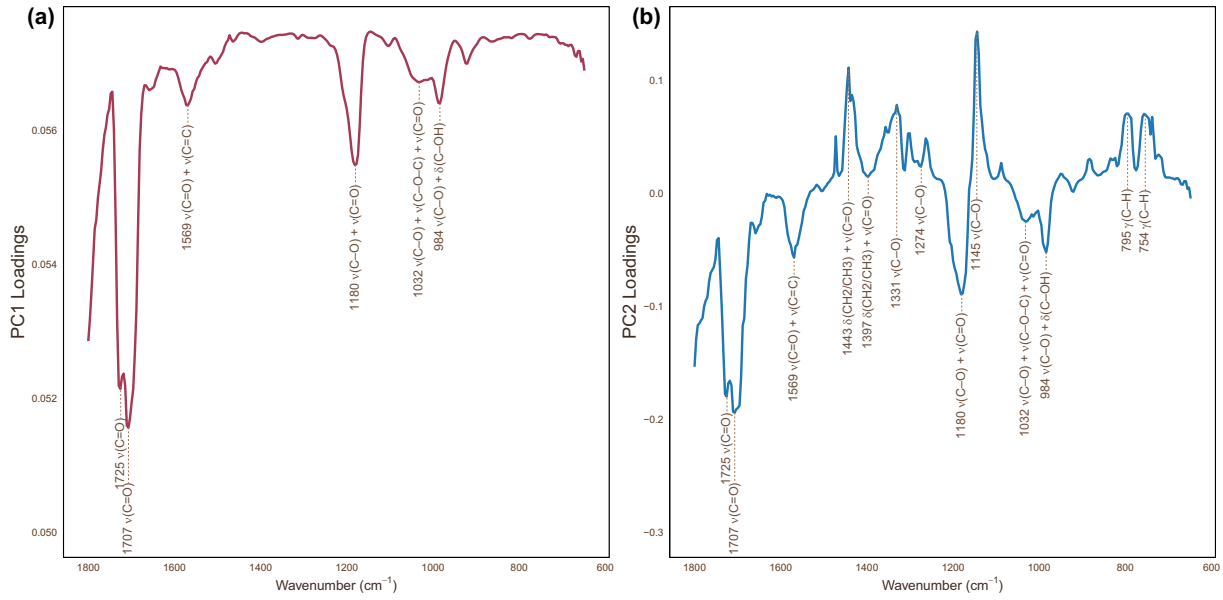

Fig. 4. PCA loadings of FT-IR spectra for coffee pulp samples, showing the contribution of molecular bands to the principal components. (a) PC1 loadings and (b) PC2 loadings.

drying, oven-drying, and roasting). Unlike the previous exploratory analysis, this supervised approach focused on maximizing group separation, identifying the most relevant bands for each condition. These bands reflect potential changes in the structural and metabolic composition of the lignocellulosic matrix and its secondary metabolites.

All VIP bands are shown as individual wavenumbers in Fig. 6 and Supplementary Table S2. Both the figure and table indicate whether each band was important for ripeness discrimination (purple), drying method (blue), or both factors (yellow). In the discussion, however, they are presented as ranges when adjacent wavenumbers correspond to the same spectral peak, to reflect their interpretation as unified vibrational features rather than separate signals.

The bands contributing most to ripeness discrimination are associated with the presence and transformation of lignin, cellulose, hemicellulose, and secondary metabolites such as chlorogenic acids (Barrios-Rodríguez et al., 2021; Jiménez-Ochoa et al., 2022; Liang et al., 2016; Oliveira et al., 2018; Yu et al., 2025; Zeleke et al., 2022). In particular, the band at 1550.6 cm^{-1} may be linked to progressive modifications of

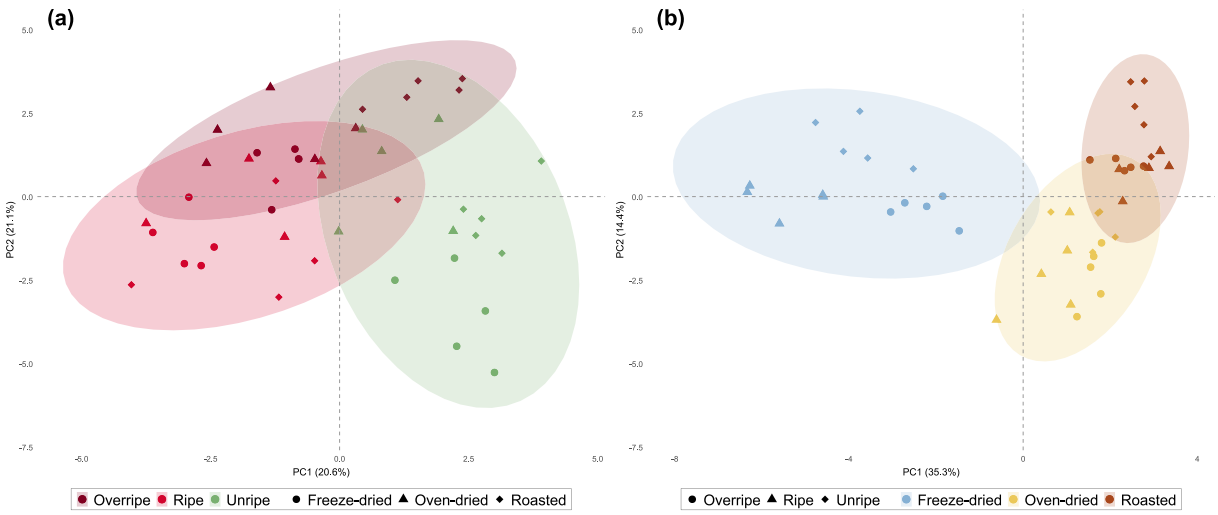

Fig. 5. sPLS-DA model applied to IR spectroscopy to classify coffee pulp samples by (A) Ripeness stage, and (B) Drying method.

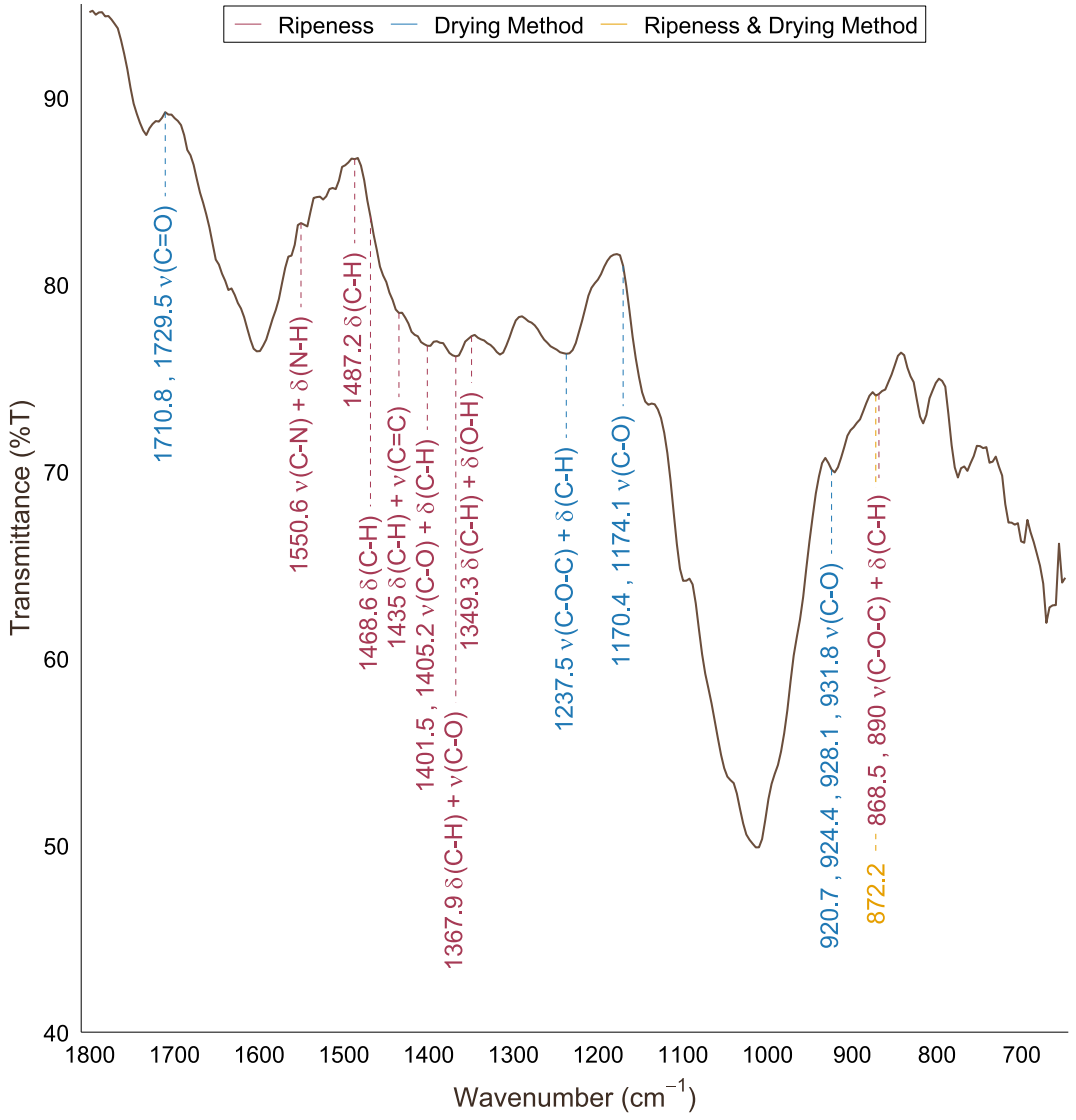

Fig. 6. VIP scores of IR bands and their relevance in discriminating ripeness (purple), drying method (blue), and the ripeness/drying interaction for coffee pulp (yellow). (For interpretation of the references to color in this figure legend, the reader is referred to the web version of this article.)

lignin and structural proteins during over-ripening. This process is likely promoted by the activity of polyphenol oxidases and peroxidases which promote the oxidation of phenolic compounds and the partial breakdown of lignocellulose (de Silva et al., 2023). Bands between 1349.3 and 1487.2 cm^{-1} associated with chlorogenic acids (Jiménez-Ochoa et al., 2022; Liang et al., 2016; Yu et al., 2025), likely reflect enzymatic hydrolysis and non-enzymatic oxidation processes that could reduce their content in overripe pulp (Farah & Donangelo, 2006). This suggests a detrimental effect on antioxidant capacity, as will be detailed later in this work.

The bands with the highest discriminant value for thermal treatments (Table S2) reflect structural modifications induced by freeze-drying, oven-drying, and roasting. Freeze-drying favored the preservation of the lignocellulosic structure, while oven-drying and roasting promoted the degradation of carbohydrates and phenolic compounds, as evidenced by the increase in signals associated with carbonyls and volatile esters. Bands at 1710.8 and 1729.5 cm^{-1} indicated the generation of carboxylic acids, volatile esters, and lactones, typical products of carbohydrate and lignin pyrolysis under severe thermal treatment (Belchior et al., 2020; Zeleke et al., 2022). Bands between 1170.4 and 1237.5 cm^{-1}, linked to oxygenated fragments derived from lignin, chlorogenic acids, and caffeine, may reflect thermal degradation and the induction of carbonyl-rich structure formation (Barrios-Rodríguez et al., 2021; Oliveira et al., 2018). Finally, bands between 920.7 and 931.8 cm^{-1} suggest thermal alterations in polysaccharides such as galactomannans and 3,6-anhydro-galactopyranose residues (Belchior et al., 2020).

The band at 872.2 cm^{-1} was relevant for both ripeness and drying, reflecting structural changes in lignocellulosic components. This signal, associated with glycosidic ring vibrations in cellulose and hemicellulose, suggests that physiological ripening processes and thermal dehydration-induced modifications affect similar structures. During ripening, changes in the proportion of these polysaccharides may alter spectral intensity, while thermal treatments likely promote glycosidic bond cleavage or structural rearrangements (Veiga et al., 2017). These results position the 872.2 cm^{-1} band as a sensitive marker of both physiological and thermal transformations.

In general, the VIP analysis identified key structural modifications occurring both during physiological ripening and thermal processing. Ripeness discrimination was supported by changes in the plant cell wall, associated with the reorganization of lignin, cellulose, and hemicellulose, as well as transformations of phenolic metabolites such as chlorogenic acids. In contrast, the bands relevant for drying treatments reflected typical thermal modifications, including the oxidation of phenolic compounds, decomposition of polysaccharides and lignin, and the formation of carbonyls and volatile esters. Unlike the gradual changes observed during ripening, thermal treatments induced deeper modifications in the chemical architecture of the pulp.

Furthermore, the FT-IR analysis, including general spectral characterization, PCA loadings, and VIP discriminants, revealed that carbonyl groups (1700–1730 cm^{-1}), aromatic structures associated with lignin and phenolic compounds (1300–1600 cm^{-1}), and glycosidic and polysaccharide-related bands (900–1200 cm^{-1}) were the primary markers differentiating coffee pulp samples according to ripening stage and thermal processing. This integrated spectral approach highlighted the combined effects of physiological maturation and drying treatments on the chemical structure and functional potential of the pulp matrix.

In summary, these FT-IR findings provide a solid foundation for interpreting subsequent changes in antioxidant activity and the bioactive metabolite profile, demonstrating that both fruit ripeness and processing type significantly impact the chemical organization of the matrix. These aspects will be explored in the following sections.

3.2. Effect of ripening and drying on coffee pulp bioactive profile

Table 1 summarizes the average values of antioxidant capacity (ABTS and DPPH), total phenolic content (TPC), caffeine (CAF), trigonelline (TRG), and chlorogenic acid (5-CQA) in coffee pulp extracts from the Catimor variety. The data are classified by fruit ripening stage (unripe, ripe, and overripe) and drying method (freeze-drying, oven-drying, and roasting). Both factors significantly influenced most of the evaluated variables ($p < 0.05$), indicating that ripening and thermal processing jointly modulate the bioactive composition of coffee pulp. Table 2 is presented as the main data source, containing the full statistical comparisons, while Fig. 7 serves as a complementary visual tool to enhance interpretation of trends and interactions. For clarity, the results are described by drying method, highlighting the primary effect of thermal treatment and the associated variations within each ripening stage. The following sections detail the specific responses of each variable, emphasizing treatments that positively or negatively impacted the functional profile of this by-product.

Numerous studies have reported substantial variability in the antioxidant capacity and bioactive compound content of coffee pulp, attributed to factors such as species and variety, geographical origin, cultivation practices, ripening stage, post-harvest handling, extraction method and analytical techniques. The reported ranges for ABTS, DPPH, TPC, caffeine, trigonelline, and 5-CQA are summarized in Table 2. Among the evaluated compounds, total phenolics and chlorogenic acids stand out for their high variability in the literature, with common values ranging from 5 to 50 mg/g and approximately 2 mg/g, respectively. Although higher values are less frequent, they are not considered atypical. Given the multifactorial influences on these variables, freeze-dried samples serve as a critical baseline for assessing the isolated effect of ripening, free from thermal processing interference. Consequently, freeze-dried samples are used as a reference to evaluate the impact of oven-drying and roasting, while unripe pulp samples provide the baseline for maturity comparisons.

3.2.1. Statistical analysis of ripening, drying method, and their interaction effects

The statistical analysis revealed distinct effects depending on the evaluated factor (see Fig. 7a and Table 2). Ripening significantly influenced DPPH ($p = 0.029$), caffeine ($p \approx 2.96 \times 10^{-5}$), trigonelline ($p = 0.0017$), and 5-CQA ($p = 0.0135$), while no significant differences were observed for ABTS and TPC. Drying had a significant impact on all variables except caffeine (ABTS $p = 1.34 \times 10^{-8}$; DPPH $p = 0.035$; TPC $p \approx 1.79 \times 10^{-10}$; trigonelline $p = 0.0048$; 5-CQA $p = 0.0055$; caffeine $p = 0.6071$). Furthermore, a significant ripening × drying interaction was detected for ABTS ($p = 0.000692$), DPPH ($p \approx 0.006$), and 5-CQA ($p \approx 2.635 \times 10^{-8}$), but not for TPC, caffeine, or trigonelline (see Fig. 8).

3.2.1.1. Ripening effect on bioactive compounds. Ripening induced contrasting changes in the bioactive profile, reflecting distinct biochemical dynamics at each fruit development stage. ABTS and TPC values remained stable across ripening stages, with no significant differences observed (Fig. 7b). The biochemical and structural factors inherent to the plant tissue may explain this apparent stability. Firstly, degradation of free phenolics such as chlorogenic acids, which typically decrease at advanced maturity stages, is counterbalanced by the accumulation of stable polymeric compounds (e.g., condensed tannins) and formation of new antioxidant species through enzymatic oxidation (e.g., quinones and phenolic polymers) (Bastian et al., 2021; Farah & Donangelo, 2006). Simultaneously, compensatory mechanisms, such as retention of cell wall-bound phenolics, support overall antioxidant capacity. Additionally, the carbohydrate- and pectin-rich matrix physically protects these compounds from degradation. Moreover, the methodological limitations of TPC and ABTS assays, namely their inability to differentiate between free and polymerized phenolics, may obscure subtle changes in bioactive fractions, contributing to the observed stability (Apak et al., 2016; Mercado-Mercado et al., 2020; Shi et al., 2024).

In contrast, DPPH scavenging capacity decreased from unripe to ripe

Table 2
Content of antioxidant parameters (ABTS, DPPH, TPC) and bioactive compounds (caffeine, trigonelline, 5-CQA) in coffee pulp as affected by ripening stage and drying method.

n		ABTS (μmol/g)	DPPH (μmol/g)	TPC (mg/g)	CAF (mg/g)	TRG (mg/g)	5-CQA (mg/g)
Unripe	Freeze-dried	94.13 ± 10.98 Aa	81.91 ± 4.61 ABa	20.53 ± 1.23 Aa	9.32 ± 0.11 Aa	6.75 ± 0.30 Aa	3.15 ± 0.52 Aa
	Oven-dried	55.27 ± 2.61 Ab	31.43 ± 2.30 ABb	13.86 ± 1.22 Ab	8.54 ± 0.47 Aa	6.89 ± 0.35 Aa	1.60 ± 0.16 Ab
	Roasted	125.79 ± 1.04 Ac	57.13 ± 1.55 ABab	27.81 ± 0.66 Ac	9.49 ± 0.21 Aa	9.31 ± 0.40 Ab	2.11 ± 0.18 Ab
Ripe	Freeze-dried	96.78 ± 12.19 Aa	50.88 ± 7.80 Aa	22.88 ± 3.37 Aa	8.17 ± 0.08 Aa	5.22 ± 0.25 ABa	5.82 ± 0.41 ABa
	Oven-dried	51.68 ± 5.19 Ab	38.20 ± 2.61 Ab	11.34 ± 1.27 Ab	8.18 ± 0.07 Aa	5.87 ± 0.29 ABa	1.08 ± 0.00 ABb
	Roasted	97.41 ± 7.84 Ac	38.20 ± 2.61 Aab	23.53 ± 0.54 Ac	8.31 ± 0.21 Aa	8.19 ± 0.37 ABb	1.08 ± 0.00 ABb
Overripe	Freeze-dried	81.00 ± 7.40 Aa	54.26 ± 5.47 Ba	18.98 ± 1.74 Aa	7.19 ± 0.17 Ba	5.19 ± 0.24 Ba	1.45 ± 0.40 Ba
	Oven-dried	64.55 ± 5.10 Ab	62.97 ± 7.02 Bb	12.14 ± 1.01 Ab	7.07 ± 0.16 Ba	5.03 ± 0.23 Ba	1.08 ± 0.00 Bb
	Roasted	98.17 ± 5.01 Ac	72.78 ± 10.00 Bab	22.28 ± 0.61 Ac	7.14 ± 0.11 Ba	6.12 ± 0.28 Bb	1.08 ± 0.00 Bb
Reported ranges for *Coffea Arabica* Pulp		20–350[1]	20–140[2]	5–300[3]	2–10[4]	1–11[5]	0.1–12[6]

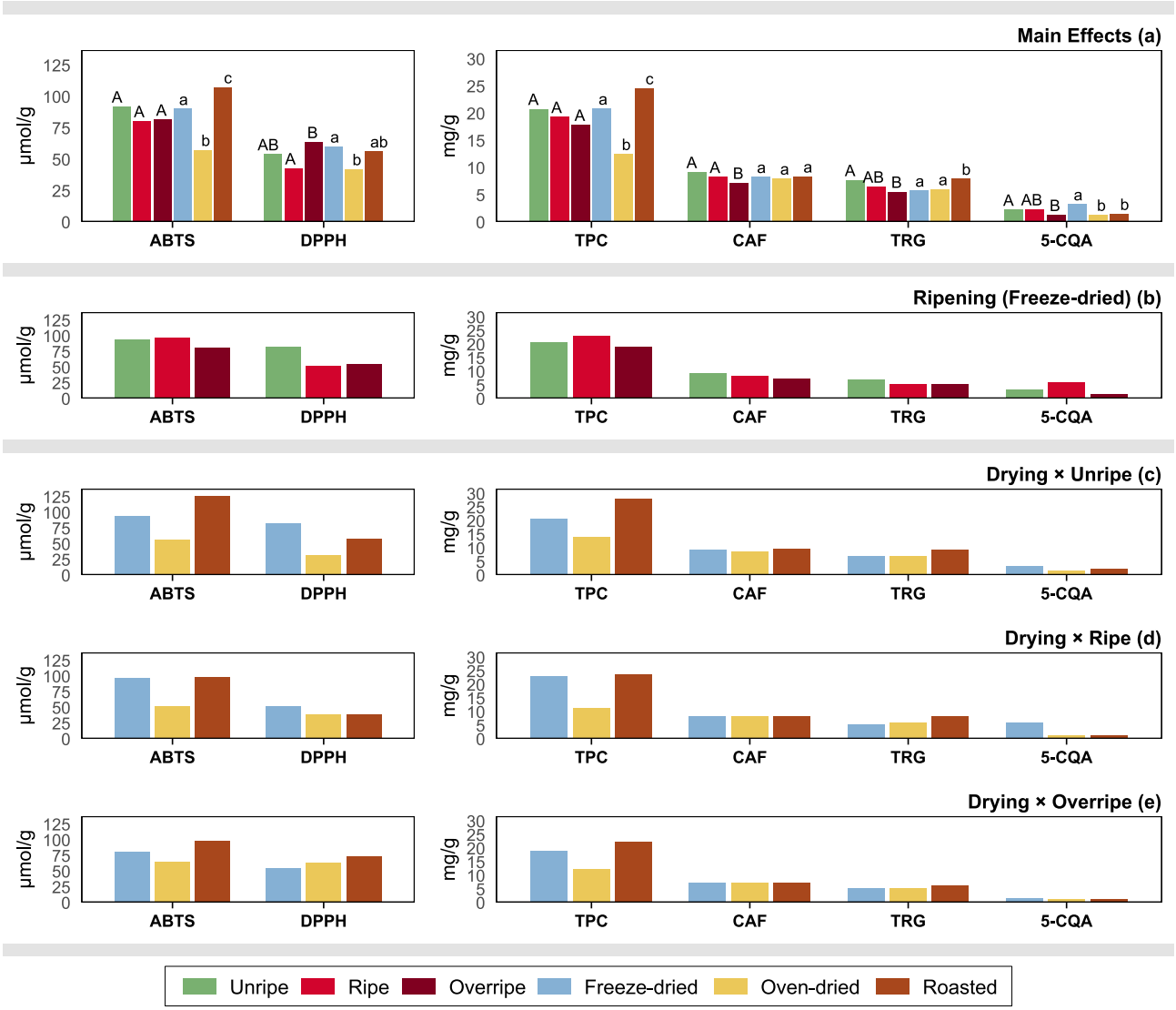

Fig. 7. Antioxidant capacity (ABTS, DPPH), total phenolic content (TPC), caffeine (CAF), trigonelline (TRG), and 5-caffeoylquinic acid (5-CQA) in coffee pulp extracts as influenced by ripening stage (unripe, ripe, overripe) and drying method (freeze-drying, oven-drying, roasting). The figure includes five panels: (a) main effects of ripening and drying; (b) effect of ripening stage evaluated in freeze-dried samples; (c) effect of drying method on unripe pulp; (d) effect of drying method on ripe pulp; and (e) effect of drying method on overripe pulp. Different letters indicate significant differences ($p < 0.05$): uppercase letters refer to ripening stage, lowercase letters to drying method.

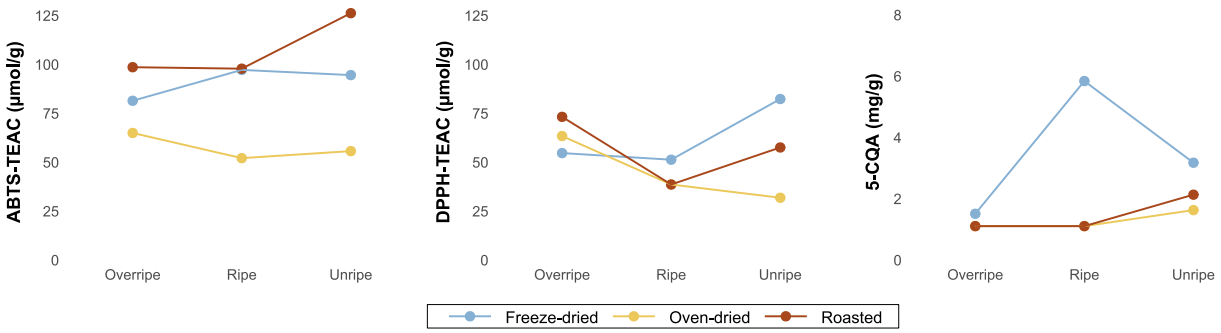

Fig. 8. Interaction effects of ripening stage and drying method on antioxidant capacity (ABTS, DPPH) and 5-CQA content in coffee pulp extracts.

stages but stabilized in overripe samples, diverging from the trends observed for ABTS and TPC. The initial decline likely reflects the loss of methanol-soluble, low-molecular-weight antioxidants, degraded by enzymatic activity and oxidative stress during early ripening. The stabilization after ripening is likely due to the accumulation of polymerized phenols, which are not effectively detected by the DPPH assay due to steric hindrance, as well as matrix-bound compounds that remain inaccessible to the extraction solvent (Apak et al., 2016; Farah & Donangelo, 2006; Myo et al., 2021). Thus, while ABTS and TPC detect the net stable antioxidant pool, DPPH only registers the loss of free, accessible phenolics.

For 5-CQA, a distinct pattern was observed: its content increased from unripe to ripe stages, followed by a marked decrease in overripeness. The initial increase may result from the hydrolysis of complex phenolic esters, such as dicaffeoylquinic acids (diCQA), generating monoesters like 5-CQA during fruit physiological maturation (Bastian et al., 2021; Farah & Donangelo, 2006). The subsequent decline in overripe samples is attributed to oxidative degradation processes affecting the free form of the compound (Bastian et al., 2021).

Caffeine content in the pulp decreased significantly from ripe to overripe stages, reflecting reduced biosynthesis and increased enzymatic degradation in the pericarp. This pattern is consistent with the metabolic prioritization of the seed (Keller et al., 1972), activation of catabolic pathways in peripheral tissues (Mazzafera et al., 1994), and downregulation of biosynthetic genes (Koshiro et al., 2007). Finally, the progressive decrease in trigonelline with ripening could be attributed to its degradation by enzymatic activity and alterations in secondary metabolism.

3.2.1.2. Drying method effect on bioactive compounds. The response of bioactive compounds to drying treatments exhibited distinct trends. Overall, ABTS, TPC, DPPH (in unripe samples), and 5-CQA decreased after oven-drying when compared to freeze-dried samples, while their levels increased considerably following roasting (Figs. 7c–e). Notably, for DPPH, this pattern was only observed in unripe samples, where roasting enabled a partial recovery, likely due to limited formation of reducing compounds (Bastian et al., 2021; Farah & Donangelo, 2006).

Oven-drying, conducted at moderate temperature and extended duration (50 °C, ~24 h), predominantly favored degradation processes (de Farias Marques et al., 2022; Lu et al., 2023). Many phenolic and antioxidant compounds are primarily bound to the cell wall (Santos da Silveira et al., 2019). Although heat promotes their release (Gonçalves et al., 2021; Oliveira et al., 2018), the plant cell wall—composed of cellulose, hemicellulose, and lignin—requires intense thermal shocks or high temperatures for complete deconstruction. At oven-drying temperatures, only the tonoplast would be affected (Liu et al., 2019), limiting the release of these compounds. Furthermore, for thermolabile molecules such as 5-CQA, prolonged exposure (24 h) exacerbates thermal and oxidative degradation, even at low temperatures (Santos da Silveira et al., 2019), explaining the reduced levels observed in oven-dried samples, where degradation prevailed over release.

In contrast, roasting at high temperature and short duration (100 °C, 10 min) enhanced the release of bioactive compounds and the formation of new products (de Farias Marques et al., 2022; Lu et al., 2023). This process facilitates the liberation of compounds from deeper layers of the plant matrix, as the plasma membrane and cell wall disintegrate at this temperature (Ribas-Agustí et al., 2018). During roasting, bound polyphenols are converted into free forms, promoting the release of compounds such as 5-CQA, whose degradation remains minimal due to the brief exposure; significant changes are reported only after 30 min at this temperature (Liu et al., 2019). Additionally, Maillard reactions, caramelization, and thermal degradation of phenolics lead to the formation of melanoidins and low-molecular-weight structures that contribute significantly to antioxidant capacity. These effects can even double antioxidant capacity, depending on the initial content of polyphenols, alkaloids, and varietal characteristics (Lu et al., 2023).

Antioxidant activity (DPPH) in coffee pulp exhibited contrasting patterns depending on fruit ripening and thermal treatment. Notably, ripening determines antioxidant accessibility: structural rigidity (unripe), polymerization (ripe), and porosity (overripe) (De Castro & Marraccini, 2006) modulate the efficiency of thermal treatments, highlighting the interactive effects of these factors. Specifically, in unripe samples, the rigid cell matrix limited antioxidant release during drying, favoring the degradation of sensitive compounds like 5-CQA. Roasting partially disrupted these structures, recovering some activity. In ripe samples, the absence of DPPH activity recovery suggests the formation of stable polymers (e.g., lignins or melanoidins), which DPPH cannot detect due to their limited proton/electron-donating capacity, a fundamental requirement for this assay. In overripe pulp, the already degraded and porous matrix facilitated progressive release: oven-drying initiated the breakdown of lignocellulosic polymers, while roasting further enhanced antioxidant release, reaching the highest observed value (72.78 µmol/g).

Data are presented as mean ± SD ($n = 3$). Different letters within the same row indicate significant differences ($p < 0.05$): Capital letters (A, B, C): differences among ripening stages (same column); lowercase (a, b, c): among drying methods (same row). Parametric tests (ANOVA followed by Tukey's HSD and Fisher's LSD when appropriate) were used for ABTS, TPC, and DPPH (drying method); nonparametric tests (Kruskal–Wallis followed by Dunn–Bonferroni) were applied for DPPH (ripening stage), CAF, TRG, and 5-CQA. For 5-CQA, values below the LOQ (1.08 mg/g) were replaced with the LOQ for statistical analysis and presentation; all measurements were well above the LOD. References: 1 (Delgado et al., 2019;Hasballah et al., 2022; Myo & Khat-udomkiri, 2022); 2. (Hasballah et al., 2022; Myo & Khat-udomkiri, 2022); 3.(S. Hu et al., 2023; Lu et al., 2023); 4 (S. Hu et al., 2023; Rebollo-Hernanz et al., 2023). 5. (Cangussu et al., 2021; Myo & Khat-udomkiri, 2022); 6. (Cangussu et al., 2021; Iriondo-DeHond et al., 2019; Rebollo-Hernanz et al., 2023).

Regarding caffeine, its concentration remained unaffected by thermal treatments, which aligns with its well-established stability during roasting. In contrast, trigonelline content increased exclusively after

roasting. This alkaloid is known for its thermal sensitivity, with marked degradation occurring at high temperatures (140–180 °C), where it begins converting into nicotinic acid (niacin, vitamin B3) (Casal et al., 2000). However, at moderate temperatures (~100 °C), the partial breakdown of cell walls and the dissociation of intracellular bonds facilitate the release of bound trigonelline, enhancing its availability without inducing degradation (Delgado et al., 2019; Mesfin et al., 2023). This mechanism explains the higher trigonelline content detected in roasted samples than oven-dried ones, where compound release remained limited.

3.2.1.3. Ripening × drying interaction on bioactive profiles. Fig. 8 shows the variables with a significant interaction between ripening stage and drying method, specifically antioxidant capacity (ABTS, DPPH) and 5-CQA content in coffee pulp extracts. The graphs highlight the differential response of each variable across ripening stages, illustrating how the physiological state of the tissue modulates the effectiveness of thermal treatments.

This interaction is further evidenced in Figs. 7b–e, where the behavior of each variable varies depending on the sample's maturity and the applied drying method. In particular, matrix rigidity in early stages, polymer stabilization during ripening, and increased porosity in overripe samples influenced the effectiveness of drying and roasting in releasing functional antioxidant compounds. These findings confirm that the drying effect cannot be assessed independently, as ripening fundamentally conditions bioactive metabolites' release, stability, and transformation. Consequently, the interaction between ripening and drying methods plays a decisive role in shaping the functional expression of coffee pulp, reinforcing the need to consider this combined effect in developing valorization strategies for this by-product.

Overall, the results confirm that the bioactive compound responses in coffee pulp are modulated by fruit ripening and drying conditions, highlighting each factor's distinct role in metabolite stability, transformation, and release. Freeze-drying proved the most effective method for preserving antioxidant capacity and bioactive compound content. At the same time, thermal processes revealed a critical balance between compound release and degradation, the extent of which depends on tissue characteristics. It is thus confirmed that the impact of drying cannot be evaluated in isolation, as ripening decisively influences the susceptibility of metabolites to undergo structural and functional transformations. These findings reinforce the need to consider the interaction between ripening and processing as a key factor in designing valorization strategies for coffee pulp to maximize its bioactive profile.

These findings underscore the importance of applying a multivariate approach that integrates spectroscopic and compositional data to understand the impact of processing treatments comprehensively.

3.2.2. Multivariate analysis of bioactive composition

3.2.2.1. Principal component analysis (PCA) of bioactive data. PCA was used as a dimensionality reduction tool to explore and visualize multivariate relationships among the applied treatments, based on the six measured chemical variables. The bidimensional plot (PC1 vs. PC2) allowed the identification of natural clusters reflecting the joint influence of ripening stage and drying method on the chemical profile of coffee pulp (Fig. 9).

The first three principal components explained approximately 88.7 % of the total data variance, with PC1 accounting for 48.5 %, followed by PC2 (23.8 %) and PC3 (16.4 %). The corresponding loadings indicated that PC1 was mainly influenced by caffeine (−0.41), trigonelline (−0.44), and total phenolics (−0.53), while PC2 was associated with antioxidant capacity (DPPH: 0.61; ABTS: 0.18), suggesting that these methods capture distinct antioxidant mechanisms. PC3 highlighted the importance of chlorogenic acid (5-CQA: 0.76), indicating the existence of latent axes that represent differentiated bioactive profiles.

In the PC1 vs. PC2 score plot, sample clustering was primarily driven by the drying method. Freeze-dried samples, such as VL1 (−1.34 in PC1, 0.87 in PC2) and ML1 (−1.09 in PC1, 1.51 in PC2), were located in the negative PC1 and positive PC2 region, indicating high preservation of bioactive compounds and elevated antioxidant capacity. In contrast, roasted samples such as VT1 (−3.26 in PC1, −0.94 in PC2) and MT1 (−0.93 in PC1, −1.58 in PC2) grouped in the opposite quadrant, suggesting that thermal exposure in this treatment led to partial degradation of compounds like chlorogenic acids and antioxidants.

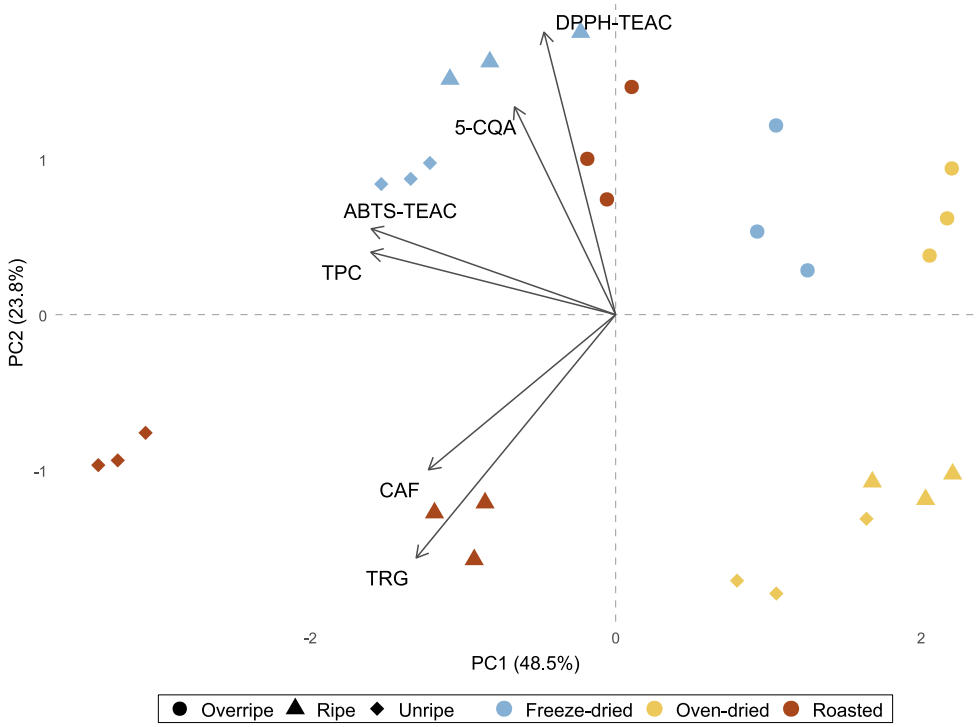

Fig. 9. Principal component analysis (PCA) of spectrophotometric and chromatographic data grouped by ripening stage and drying method of coffee pulp.

The multivariate space also revealed interesting patterns related to ripening. A closer inspection of the PC1 vs. PC2 plot showed that both unripe (VL1: –1.34; VL2: –1.53; VL3: −1.22 in PC1) and ripe samples (ML1: –1.09; ML2: –0.82; ML3: −0.23 in PC1) exhibited similar dispersion, indicating comparable variability in their chemical composition. However, overripe samples showed a distinct behavior, forming a more compact cluster (SML1: 1.26; SML2: 0.93; SML3: 1.05 in PC1), which may reflect greater biochemical homogeneity at this final stage of fruit development.

This dispersion pattern suggests that metabolic variability does not decrease linearly with ripeness but appears to stabilize in the late stages. While unripe and ripe samples, despite their physiological differences, exhibit similar fluctuations in bioactive profiles, only in the overripe stage does a more defined consolidation of chemical traits emerge, likely due to the culmination of key metabolic processes. A similar trend was observed, as reported by Bi et al. (2024), where a PCA of coffee cherries at five ripening stages revealed no clear separation between green and orange-red beans, suggesting slow changes in metabolite composition during early ripening. However, significant separation emerged among dark-red, purple-red, and purple-black groups (overripe cherries), indicating a rapid developmental phase marked by intense metabolic shifts. These findings indicate that variability does not decline linearly during maturation (Bi et al., 2024).

Altogether, the PCA analysis demonstrates that both drying method and ripening stage significantly influence the bioactive profile of coffee pulp. Compared to PLS-DA, which prioritizes variables using VIP scores, PCA reveals unsupervised clustering primarily shaped by the drying method. At the same time, PLS-DA confirms these patterns and adds a hierarchical ranking of variables (e.g., caffeine and trigonelline as key markers for ripening). The visualization of the first two components, along with the loadings plot, provides a clear understanding of the underlying data structure and supports the identification of processing strategies to preserve or transform key compounds.

3.2.2.2. PLS-DA for ripeness stage discrimination. The PLS-DA model effectively classified samples by ripening stage (green, ripe, and overripe), explaining over 87 % of X variance and nearly 100 % of Y. Score and loading plots showed progressive separation, reflecting compositional transitions during ripening. In the score plot, green samples clustered at the negative end of the first component, associated with high levels of caffeine (VIP: 1.62) and trigonelline (VIP: 1.11). In contrast, overripe samples were positioned at the positive end, reflecting a differentiated profile dominated by antioxidant activity (DPPH: VIP 0.83). Ripe samples occupied intermediate positions; however, those subjected to freeze-drying tended to group closer to green samples due to their retention of chlorogenic acid (5-CQA: VIP 0.70).

Caffeine and trigonelline were the most relevant markers, while antioxidant-related variables (ABTS, TPC) showed lower VIP scores, indicating less variation across ripening stages. Despite signs of overfitting ($Q^2 = -1.96$), the model achieved low classification error (10.81 %) and high AUC-ROC values (0.97 for green, 1.0 for overripe), confirming its capacity to capture ripening-associated patterns. These findings support the role of caffeine and trigonelline as ripeness indicators, with potential applications in quality control and traceability of coffee pulp-derived products.

3.2.2.3. PLS-DA for drying method discrimination. The PLS-DA analysis of drying methods (Fig. 10B)—freeze-drying, oven-drying, and roasting—revealed a strong impact on the chemical profile of coffee pulp. The model explained ~87 % of X variance and nearly 100 % of Y, showing excellent discrimination. The score plot displayed clear separation among treatments along the first two components.

Roasted samples clustered at the negative end of Comp. 1, associated with elevated ABTS activity (VIP = 1.32) and total phenolics (VIP = 1.37). Freeze-dried samples, grouped at the positive end of Comp. 2, preserved chlorogenic acid and DPPH activity (VIP = 0.65). Oven-dried samples occupied intermediate positions, showing less effective bioactive retention.

VIP analysis identified total phenolics and ABTS as the main discriminants among drying methods (VIP > 1), emphasizing the role of thermal treatment in modulating phenolic stability. This aligns with previous studies (D. Hu et al., 2023; Kieu Tran et al., 2020), which also highlighted the link between antioxidant behavior and processing. In contrast, caffeine showed low sensitivity to drying (VIP = 0.28), consistent with reports that roasting may slightly increase its concentration, unlike more labile phenolics (Villota et al., 2022).

Model performance was robust, with low classification error (5.48 %) and excellent AUC values: 1.0 for roasted and oven-dried samples, and 0.94 for freeze-dried ones. These results support the use of PLS-DA for exploring thermal effects on bioactive composition.

In conclusion, drying method is a critical determinant of bioactive compound preservation or transformation (D. Hu et al., 2023; Kieu Tran et al., 2020). Combined with PCA results, the findings suggest that thermal drying primarily affects phenolic compounds (D. Hu et al., 2023; Jiamjariyatam et al., 2022). Freeze-drying is recommended to retain thermolabile compounds like 5-CQA (D. Hu et al., 2023), while

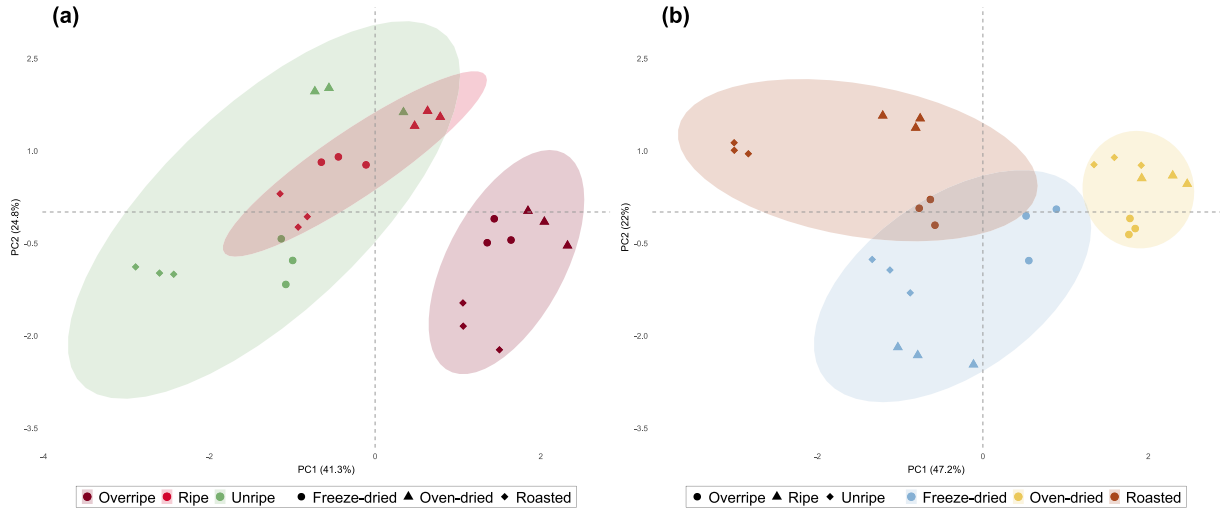

Fig. 10. Sparse partial least squares discriminant analysis (sPLS-DA) of spectrophotometric and chromatographic data to classify coffee pulp samples according to (A) ripening stage and (B) drying method.

roasting enhances ABTS activity through formation of non-phenolic antioxidants such as melanoidins, although at the cost of phenolic degradation. While the findings are derived from a single harvest and growing region, they provide a structured foundation for understanding how drying modulates bioactive profiles in coffee pulp, an essential step toward guiding functional and nutraceutical applications.

4. Conclusions

This study demonstrates, under controlled conditions, that the interaction between ripening stage and drying method can significantly modulate the bioactive profile and antioxidant capacity of *Coffea arabica* var. Catimor pulp. These factors acted synergistically, revealing that thermal processing outcomes depend not only on temperature, but also on exposure time and tissue susceptibility. Although both oven-drying and roasting produced contrasting effects: oven-drying at mild temperature but extended duration led to marked degradation of thermolabile compounds such as 5-caffeoylquinic acid (5-CQA), while roasting, conducted at moderate temperature and short duration, preserved or even enhanced certain bioactives, likely through partial matrix disruption and the formation of Maillard-derived antioxidants. In contrast, freeze-drying, which avoids thermal stress, proved the most effective for retaining native compounds.

FT-IR spectroscopy, combined with PCA and sPLS-DA, enabled the identification of spectral markers indicative of both ripeness and thermal transformations. Key signals associated with lignin and structural carbohydrates, including the region around 1170 cm^{-1}, reflected drying and ripening induced transformations, while the 872 cm^{-1} band emerged as a sensitive indicator of both physiological and thermal effects. These findings reinforce the value of FT-IR as a rapid, non-destructive tool for quality control and process monitoring in coffee pulp, and warrant further validation across broader biological and environmental contexts to establish the robustness of the observed patterns.

From a compositional perspective, roasted unripe pulp showed the highest functional potential due to enhanced release and neoformation of antioxidants, while ripe freeze-dried pulp best preserved thermolabile bioactives. These results emphasize that drying effects must be interpreted in light of ripening stage, reinforcing the need for adaptive protocols—e.g., freeze-drying for ripe pulp and controlled roasting for unripe or overripe pulp—to optimize functional quality.

Altogether, this work lays a foundation for the optimized valorization of coffee pulp as a high-value ingredient in food and nutraceutical applications. While based on a single harvest and geographic origin, the experimental design allowed for the controlled exploration of ripening and drying effects. Future studies should aim to identify and quantify specific thermal derivatives—such as melanoidins—and assess the industrial scalability of proposed treatments. The integrative approach applied here—combining multivariate spectroscopy with targeted compositional profiling—provides a valuable proof-of-concept for the analytical characterization of coffee pulp. Its contribution to circular strategies should be further explored across diverse temporal, varietal, and agroecological contexts.

Declaration of generative AI in scientific writing

During the preparation of this manuscript, generative AI tools (specifically ChatGPT, Deepseek and Quillbot) were used solely to enhance the clarity and fluency of the English language, including translation, proofreading and language polishing of our own original text, and not for content generation or idea development. All edits and suggestions provided by the tool were carefully reviewed and revised by the authors. The authors remain fully responsible for the content of the manuscript.

CRediT authorship contribution statement

Alicia María Rendón-Mera: Writing – review & editing, Writing – original draft, Validation, Supervision, Methodology, Investigation, Formal analysis, Data curation. **Carolina Vega-Oliveros:** Writing – review & editing, Writing – original draft, Validation, Supervision, Methodology, Investigation, Conceptualization. **Sandrith Ordoñez-Lozano:** Writing – original draft, Methodology, Investigation. **Daniela Martínez López:** Writing – original draft, Methodology, Investigation. **Nelson Gutiérrez Guzmán:** Supervision, Resources, Project administration, Funding acquisition.

Funding

This research was developed within the framework of the project "Generation of new knowledge in the processing and transformation of specialty coffees packaged in biodegradable materials to improve the quality of the coffee industry in the department of Huila" (BPIN 2021000100380), funded by the Colombian General System of Royalties and co-financed by the Government of Huila (Gobernación del Huila). The study was supported by the project's infrastructure and carried out at the South Colombian Center for Coffee Research (Centro Surcolombiano de Investigación en Café, Cesurcafé), part of Universidad Surcolombiana.

Declaration of competing interest

The authors declare the following financial interests/personal relationships which may be considered as potential competing interests: Alicia Maria Rendon-Mera reports financial support, administrative support, and equipment, drugs, or supplies were provided by Colombian General System of Royalties. Alicia Maria Rendon-Mera reports financial support, administrative support, and equipment, drugs, or supplies were provided by Government of Huila. Carolina *V*ega Oliveros reports financial support, administrative support, equipment, drugs, or supplies, and travel were provided by Colombian General System of Royalties. Carolina Vega Oliveros reports financial support, administrative support, equipment, drugs, or supplies, and travel were provided by Government of Huila. Sandrith Ordonez-Lozano reports financial support, administrative support, and equipment, drugs, or supplies were provided by Colombian General System of Royalties. Sandrith Ordonez-Lozano reports financial support, administrative support, and equipment, drugs, or supplies were provided by Government of Huila. Daniela Martinez Lopez reports financial support, administrative support, and equipment, drugs, or supplies were provided by Colombian General System of Royalties. Daniela Martinez Lopez reports financial support, administrative support, and equipment, drugs, or supplies were provided by Government of Huila. Nelson Gutierrez Guzman reports administrative support, equipment, drugs, or supplies, and travel were provided by Colombian General System of Royalties. Nelson Gutierrez Guzman reports administrative support, equipment, drugs, or supplies, and travel were provided by Government of Huila. If there are other authors, they declare that they have no known competing financial interests or personal relationships that could have appeared to influence the work reported in this paper.

Acknowledgments

The authors sincerely thank Marlon Bolaños, coffee grower from « Finca Varietales Exóticos » located in La Siberia, Acevedo (Huila, Colombia), for providing the *Coffea arabica* var. Catimor cherries used in this study. We are also grateful to Cesurcafé for providing access to its facilities, which enabled all postharvest and pulp processing operations, and to the dedicated staff and collaborators linked to Cesurcafé for their valuable technical assistance. Special thanks are extended to the entire project team for their commitment and support throughout the

development of this research.

Appendix A. Supplementary data

Supplementary data to this article can be found online at https://doi.org/10.1016/j.fochx.2025.102828.

Data availability

Data will be made available on request.

References

Apak, R., Özyürek, M., Güçlü, K., & Çapanoŀlu, E. (2016). Antioxidant activity/capacity measurement. 1. Classification, physicochemical principles, mechanisms, and electron transfer (ET)-based assays. *Journal of Agricultural and Food Chemistry, 64*(5), 997–1027. https://doi.org/10.1021/acs.jafc.5b04739

Barrios-Rodríguez, Y., Collazos-Escobar, G. A., & Gutiérrez-Guzmán, N. (2021). ATR-FTIR for characterizing and differentiating dried and ground coffee cherry pulp of different varieties (Coffea Arabica L.). *Engenharia Agrícola, 41*(1), 70–77. https://doi.org/10.1590/1809-4430-eng.agric.v41n1p70-77/2021

Bastian, F., Hutabarat, O. S., Dirpan, A., Nainu, F., Harapan, H., Emran, T. B., & Simal-Gandara, J. (2021). From plantation to cup: Changes in bioactive compounds during coffee processing. *Foods, 10*(11), 2827. https://doi.org/10.3390/foods10112827

Belchior, V., Botelho, B. G., Casal, S., Oliveira, L. S., & Franca, A. S. (2020). FTIR and Chemometrics as effective tools in predicting the quality of specialty coffees. *Food Analytical Methods, 13*(1), 275–283. https://doi.org/10.1007/s12161-019-01619-z

Bi, X., Yu, H., Hu, F., Fu, X., Li, Y. Y., Li, Y. Y., … Dong, W. (2024). A systematic analysis of the correlation between flavor active differential metabolites and multiple bean ripening stages of Coffea arabica L. *Molecules, 29*(1), 180. https://doi.org/10.3390/MOLECULES29010180/S1

Cangussu, L. B., Melo, J. C., Franca, A. S., & Oliveira, L. S. (2021). Chemical characterization of coffee husks, a by-product of Coffea arabica production. *Foods, 10*(12), 3125. https://doi.org/10.3390/foods10123125

Casal, S., Oliveira, M. B., & Ferreira, M. A. (2000). HPLC/diode-array applied to the thermal degradation of trigonelline, nicotinic acid and caffeine in coffee. *Food Chemistry, 68*(4), 481–485. https://doi.org/10.1016/S0308-8146(99)00228-9

De Castro, R. D., & Marraccini, P. (2006). Cytology, biochemistry and molecular changes during coffee fruit development. *Brazilian Journal of Plant Physiology, 18*(1), 175–199. https://doi.org/10.1590/S1677-04202006000100013

Delgado, S. R., Arbelaez, A. F. A., & Rojano, B. (2019). Antioxidant capacity, bioactive compounds in coffee pulp and implementation in the production of infusions. *Acta Scientiarum Polonorum. Technologia Alimentaria, 18*(3), 235–248. https://doi.org/10.17306/J.AFS.0663

Farah, A., & Donangelo, C. M. C. M. (2006). Phenolic compounds in coffee. *Brazilian Journal of Plant Physiology, 18*(1), 23–36. https://doi.org/10.1590/S1677-04202006000100003

de Farias Marques, A. D. J., de Lima Tavares, J., de Carvalho, L. M., Leite Abreu, T., Alves Pereira, D., Moreira Fernandes Santos, M., … Kênia Alencar Bezerra, T. (2022). Oxidative stability of chicken burgers using organic coffee husk extract. *Food Chemistry, 393*, Article 133451. Contents https://doi.org/10.1016/j.foodchem.2022.133451.

Gonçalves, B. M. M., de Camillo, M. O., Oliveira, M. P., Carreira, L. G., Moulin, J. C., Neto, H. F., … Monteiro, S. N. (2021). Surface treatments of coffee husk fiber waste for effective incorporation into polymer biocomposites. *Polymers, 13*(19), 3428. https://doi.org/10.3390/polym13193428

Hasballah, K., Lestari, W., Listiawan, M. Y., & Sofia, S. (2022). Coffee by-products as the source of antioxidants: A systematic review. In *, 11. F1000Research*. F1000 research ltd.. https://doi.org/10.12688/f1000research.107811.1

Hu, D., Liu, X., Qin, Y., Yan, J., Li, R., & Yang, Q. (2023). The impact of different drying methods on the physical properties, bioactive components, antioxidant capacity, volatile components and industrial application of coffee peel. *Food Chemistry: X, 19*, Article 100807. https://doi.org/10.1016/J.FOCHX.2023.100807

Hu, S., Gil-Ramírez, A., Martín-Trueba, M., Benítez, V., Aguilera, Y., & Martín-Cabrejas, M. A. (2023). Valorization of coffee pulp as bioactive food ingredient by sustainable extraction methodologies. *Current Research in Food Science, 6*, Article 100475. https://doi.org/10.1016/J.CRFS.2023.100475

Iriondo-DeHond, A., Aparicio García, N., Fernandez-Gomez, B., Guisantes-Batan, E., Velázquez Escobar, F., Blanch, G. P., … del Castillo, M. D. (2019). Validation of coffee by-products as novel food ingredients. *Innovative Food Science and Emerging Technologies, 51*, 194–204. https://doi.org/10.1016/j.ifset.2018.06.010

Jiamjariyatam, R., Samosorn, S., Dolsophon, K., Tantayotai, P., Lorliam, W., & Krajangsang, S. (2022). Effects of drying processes on the quality of coffee pulp. *Journal of Food Processing and Preservation, 46*(10), Article e16876. https://doi.org/10.1111/JFPP.16876

Jiménez-Ochoa, J. P., Barrios-Rodríguez, Y. F., Bahamón-Monje, A. F., & Gutiérrez-Gúzman, N. (2022). Physicochemical and sensory characteristics of dehydrated coffee pulp in function of drying temperature. *Revista Brasileira de Engenharia Agricola e Ambiental, 26*(12), 894–900. https://doi.org/10.1590/1807-1929/AGRIAMBI.V26N12P894-900

Keller, H., Wanner, H., & Baumann, T. W. (1972). Kaffeinsynthese in Früchten und Gewebekulturen von Coffea arabica. *Planta, 108*(4), 339–350. https://doi.org/10.1007/BF00389311

Kieu Tran, T. M., Kirkman, T., Nguyen, M., & Van Vuong, Q. (2020). Effects of drying on physical properties, phenolic compounds and antioxidant capacity of Robusta wet coffee pulp (Coffea canephora). *Heliyon, 6*(7), Article e04498. https://doi.org/10.1016/j.heliyon.2020.e04498

Koshiro, Y., Jackson, M. C., Katahira, R., Wang, M. L., Nagai, C., & Ashihara, H. (2007). Biosynthesis of chlorogenic acids in growing and ripening fruits of Coffea arabica and Coffea canephora plants. *Zeitschrift Fur Naturforschung - Section C Journal of Biosciences, 62*(9–10), 731–742. https://doi.org/10.1515/znc-2007-9-1017

Král, E., Rukov, J. L., & Mendes, A. C. (2024). Coffee cherry on the top: Disserting valorization of coffee pulp and husk. *Food Engineering Reviews, 16*(1), 146–162. https://doi.org/10.1007/s12393-023-09352-4

Liang, N., Lu, X., Hu, Y., & Kitts, D. D. (2016). Application of attenuated Total reflectance-Fourier transformed infrared (ATR-FTIR) spectroscopy to determine the Chlorogenic acid isomer profile and antioxidant capacity of coffee beans. *Journal of Agricultural and Food Chemistry, 64*(3), 681–689. https://doi.org/10.1021/acs.jafc.5b05682

Liu, D., Lopez-Sanchez, P., & Gidley, M. J. (2019). Cellular barriers in apple tissue regulate polyphenol release under different food processing and: In vitro digestion conditions. *Food & Function, 10*(5), 3008–3017. https://doi.org/10.1039/c8fo02528b

Lu, T., Sun, Y., Huang, Y., & Chen, X. (2023). Effects of roasting on the chemical compositions, color, aroma, microstructure, and the kinetics of changes in coffee pulp. *Journal of Food Science, 88*(4), 1430–1444. https://doi.org/10.1111/1750-3841.16516

Mazzafera, P., Crozier, A., & Sandberg, G. (1994). Studies on the metabolic control of caffeine turnover in developing endosperms and leaves of Coffea arabica and Coffea dewevrei. *Journal of Agricultural and Food Chemistry, 42*(7), 1423–1427. https://doi.org/10.1021/jf00043a007

Mesfin, K., Gemechu, F. G., Belayneh, T., & Tessema, H. A. (2023). Coffee fruit roasting: An approach to enhance yield and bioactivities of ethanol extracts from coffee husk. *ACS Food Science & Technology, 3*(6), 1066–1076. https://doi.org/10.1021/ACSFOODSCITECH.3C00064

Myo, H., & Khat-udomkiri, N. (2022). Optimization of ultrasound-assisted extraction of bioactive compounds from coffee pulp using propylene glycol as a solvent and their antioxidant activities. *Ultrasonics Sonochemistry, 89*, Article 106127. https://doi.org/10.1016/J.ULTSONCH.2022.106127

Myo, H., Nantarat, N., & Khat-Udomkiri, N. (2021). Changes in bioactive compounds of coffee pulp through fermentation-based biotransformation using lactobacillus plantarum tistr 543 and its antioxidant activities. *Fermentation, 7*(4). https://doi.org/10.3390/fermentation7040292

de Oliveira, F. C., Srinivas, K., Helms, G. L., Isern, N. G., Cort, J. R., Gonçalves, A. R., & Ahring, B. K. (2018). Characterization of coffee (Coffea arabica) husk lignin and degradation products obtained after oxygen and alkali addition. *Bioresource Technology, 257*, 172–180. https://doi.org/10.1016/J.BIORTECH.2018.01.041

Oteef, M. D. Y. (2022). Comparison of different extraction techniques and conditions for optimizing an HPLC-DAD method for the routine determination of the content of Chlorogenic acids in green coffee beans. *Separations, 9*(12). https://doi.org/10.3390/separations9120396

Rebollo-Hernanz, M., Aguilera, Y., Gil-Ramírez, A., Benítez, V., Cañas, S., Braojos, C., & Martin-Cabrejas, M. A. (2023). Biorefinery and stepwise strategies for valorizing coffee by-products as bioactive food ingredients and nutraceuticals. *Applied Sciences, 13*(14), 8326. https://doi.org/10.3390/APP13148326

Ribas-Agustí, A., Martín-Belloso, O., Soliva-Fortuny, R., & Elez, P. (2018). Food processing strategies to enhance phenolic compounds bioaccessibility and. *Critical Reviews in Food Science and Nutrition, 58*(15), 2531–2548.

Santos da Silveira, J., Durand, N., Lacour, S., Belleville, M. P., Perez, A., Loiseau, G., & Dornier, M. (2019). Solid-state fermentation as a sustainable method for coffee pulp treatment and production of an extract rich in chlorogenic acids. *Food and Bioproducts Processing, 115*, 175–184. https://doi.org/10.1016/j.fbp.2019.04.001

de Silva, C. O. G., Vuillemin, M., Kabel, M. A., van Berkel, W. J. H., Meyer, A. S., & Agger, J. W. (2023). Polyphenol oxidase products are priming agents for LPMO Peroxygenase activity. *ChemSusChem, 16*(18), Article e202300559. https://doi.org/10.1002/CSSC.202300559

Taleb, F., Ammar, M., Mosbah, M., & ben, Salem, R. ben, & Moussaoui, Y.. (2020). Chemical modification of lignin derived from spent coffee grounds for methylene blue adsorption. *Scientific Reports, 10*(1), 1–13. https://doi.org/10.1038/s41598-020-68047-6

Veiga, T. R. L. A., Lima, J. T., de Dessimoni, A. L. A., Pego, M. F. F., Soares, J. R., & Trugilho, P. F. (2017). Different plant biomass characterizations for biochar production. *Cerne, 23*(4), 529–536. https://doi.org/10.1590/01047760201723042373

Villota, H., Santa-González, G. A., Uribe, D., Henao, I. C., Arroyave-Ospina, J. C., Barrera-Causil, C. J., & Pedroza-Díaz, J. (2022). Modulatory effect of Chlorogenic acid and coffee extracts on Wnt/β-catenin pathway in colorectal Cancer cells. *Nutrients, 14*(22). https://doi.org/10.3390/nu14224880

Yu, X., Zhu, K., Hu, F., Hu, R., & Dong, W. (2025). Effects of ultrasonic treatment on the physicochemical, structural, and functional properties of soluble dietary fiber from coffee peels. *Ultrasonics Sonochemistry, 114*, Article 107247. https://doi.org/10.1016/J.ULTSONCH.2025.107247

Zeleke, N. M., Sinha, D. K., & Mengesha, G. A. (2022). Chemical composition and extraction of Micro crystalline cellulose from outer skin isolated coffee husk. *Advances in Materials Science and Engineering, 1*, 7163359. https://doi.org/10.1155/2022/7163359